Discoidin domain receptor 1 controls linear invadosome formation via a Cdc42–Tuba pathway

Amélie Juin,[1,2]* Julie Di Martino,[1,2]* Birgit Leitinger,[3] Elodie Henriet,[1,2] Anne-Sophie Gary,[1,2] Lisa Paysan,[1,2] Jeremy Bomo,[4] Georges Baffet,[4] Cécile Gauthier-Rouvière,[5] Jean Rosenbaum,[1,2] Violaine Moreau,[1,2] and Frédéric Saltel[1,2]

[1]Institut National de la Santé et de la Recherche Médicale, U1053, F-33076 Bordeaux, France
[2]Université de Bordeaux, F-33076 Bordeaux, France
[3]National Heart and Lung Institute, Imperial College London, London SW7 2AZ, England, UK
[4]Institut National de la Santé et de la Recherche Médicale, U1085, Institut de Recherche sur la Santé l'Environnement et le Travail (IRSET), Université de Rennes 1, 35043 Rennes, France
[5]Universités Montpellier 2 et 1, Centre de Recherche de Biochimie Macromoléculaire, Centre National de la Recherche Scientifique, UMR 5237, 34293 Montpellier, France

Accumulation of type I collagen fibrils in tumors is associated with an increased risk of metastasis. Invadosomes are F-actin structures able to degrade the extracellular matrix. We previously found that collagen I fibrils induced the formation of peculiar linear invadosomes in an unexpected integrin-independent manner. Here, we show that Discoidin Domain Receptor 1 (DDR1), a collagen receptor overexpressed in cancer, colocalizes with linear invadosomes in tumor cells and is required for their formation and matrix degradation ability. Unexpectedly, DDR1 kinase activity is not required for invadosome formation or activity, nor is Src tyrosine kinase. We show that the RhoGTPase Cdc42 is activated on collagen in a DDR1-dependent manner. Cdc42 and its specific guanine nucleotide-exchange factor (GEF), Tuba, localize to linear invadosomes, and both are required for linear invadosome formation. Finally, DDR1 depletion blocked cell invasion in a collagen gel. Altogether, our data uncover an important role for DDR1, acting through Tuba and Cdc42, in proteolysis-based cell invasion in a collagen-rich environment.

Introduction

Type I collagen fibrils are present in tumors, where they were long considered to be a simple physical and structural barrier to inhibit tumor progression and metastasis. However, type I collagen is overexpressed in a large number of cancers, and, paradoxically, a high expression is correlated with an increased risk of metastasis, for instance in breast and lung cancers (Ramaswamy et al., 2003; Gilkes et al., 2013). Collagen overexpression is not the only factor involved in cancer progression. Indeed, the size, diameter, morphology, and cross-linking of type I collagen fibrils have an impact on tumor cell proliferation and metastatic growth (Levental et al., 2009; Cox et al., 2013). Moreover, type I collagen fibrils promote the activity of matrix metalloproteases (MMPs; Ruangpanit et al., 2001).

We previously discovered that type I collagen fibrils are powerful and physiological inducers of invadosomes, which are F-actin–rich structures able to degrade the ECM (Juin et al., 2012). The term invadosomes refers to podosomes in normal cells as well as to invadopodia in cancer cells. Both are matrix-degrading structures allowing matrix remodeling and cell invasion due to the activity of MMPs such as MMP2, MMP9, and MT1-MMP (Hoshino et al., 2013). Invadosomes in some cancers correlate with their ability to metastasize (Eckert et al., 2011). Moreover, invadosomes were recently involved in tumor cell extravasation and demonstrated to be a therapeutic target for metastasis (Leong et al., 2014). Invadosome formation, organization, and activation are controlled by RhoGTPases such as RhoA, Rac1, and Cdc42 (Moreau et al., 2003; Di Martino et al., 2014) and also by Src kinases (Tarone et al., 1985; Linder et al., 2000; Hauck et al., 2002). The invadosome basic module

*A. Juin and J. Di Martino contributed equally to this paper.

Correspondence to Violaine Moreau: violaine.moreau@inserm.fr; or Frédéric Saltel: frederic.saltel@inserm.fr

Abbreviations used in this paper: CMV, cytomegalovirus; DDR, Discoidin domain receptor; GAPDH, glyceraldehyde 3-phosphate dehydrogenase; GEF, guanine nucleotide-exchange factor; MMP, matrix metalloprotease; N-WASP, neuronal Wiskott–Aldrich Syndrome protein; RTK, receptor tyrosine kinase; SHG, second harmonic generation.

The Rockefeller University Press $30.00
J. Cell Biol. Vol. 207 No. 4 517–533
www.jcb.org/cgi/doi/10.1083/jcb.201404079

corresponds to a central F-actin core composed of actin-binding proteins like neuronal Wiskott–Aldrich Syndrome protein (N-WASP), the Arp2/3 complex, and cortactin, which is associated with scaffold proteins such as Tks5 (Destaing et al., 2011; Linder et al., 2011; Murphy and Courtneidge, 2011). This actin core may be surrounded by a ring of regulating proteins like integrins, vinculin, and talin. Invadosomes are found as individual items, aggregates, or organized into "rosettes" according to cellular models and context. They are constitutive in various cancer cells and in osteoclasts, but in most cell types they are absent in basal conditions, although inducible by various stimuli including cytokines (PDGF, VEGF, and TGF-β) or various compounds (phorbol esters, cytotoxic necrotizing factor 1, and sodium fluoride; Albiges-Rizo et al., 2009). Our recent data showed that type I collagen fibrils induce invadosome formation in most cell types tested, such as endothelial cells and fibroblasts. Moreover, type I collagen fibrils promoted a linear reorganization of invadopodia in cancer cell lines, which was associated with an increase in ECM-degrading activity. Invadosomes induced or reorganized by collagen I aligned along the collagen fibers, and we thus called them linear invadosomes. Two studies have confirmed the induction of linear invadosomes upon cell contact with collagen fibrils (Monteiro et al., 2013; Schachtner et al., 2013). Interestingly, although β1 integrin family members are the major receptors for type I collagen (Leitinger, 2011) and are associated with classical invadosomes in many cell types, we found that they were not necessary for linear invadosome formation (Juin et al., 2012), raising the question about the ECM receptor involved.

Discoidin domain receptors (DDRs) are a ubiquitously expressed family of receptors known to interact with collagens, in particular fibrillar collagens I–III (Shrivastava et al., 1997; Vogel et al., 1997). DDRs only bind collagens in their native physiological triple-helical conformation and do not recognize denatured collagens such as gelatin (Konitsiotis et al., 2008). The DDR receptor family belongs to the large group of receptor tyrosine kinases (RTKs) and is composed of two members, DDR1 and DDR2. Ligand interaction with DDRs promotes tyrosine autophosphorylation as with classical RTKs, although with very slow and persistent kinetics (Vogel et al., 1997). The DDRs are considered to be collagen sensors and act on tissue homeostasis, as well as on many cellular processes, including cell proliferation and differentiation, cell adhesion, cell migration, and invasion (Leitinger, 2014). These latter properties clearly connect them with cancer. Indeed, several recent studies show that the DDRs are often up-regulated in various cancers (for review see Valiathan et al., 2012). Notably, DDR1 was found overexpressed in lung and breast cancers (Barker et al., 1995; Ford et al., 2007), where a high expression level was correlated with a poor prognosis and metastasis formation (Yang et al., 2010; Valencia et al., 2012; Miao et al., 2013).

Because both DDR1 and collagen I are overexpressed in cancers and associated with metastasis development, and as type I collagen fibrils promote linear invadosome formation, we hypothesized that DDR1 could be the collagen I receptor involved in the formation of linear invadosomes and subsequent cellular invasion.

Results

DDR1 drives linear invadosome formation and activity

For this study, we selected breast cancer and lung cancer cell lines with high levels of DDR1 expression. We found that MDA-MB-231 and A549 cells, derived from human breast and lung cancers, respectively, express DDR1 (see Fig. 2 B and Fig. S2 A). We first analyzed the formation of invadopodia in these cells. As shown by dual F-actin/cortactin immunostaining on fluorescent gelatin, A549 cells do not form constitutive invadopodia, whereas MDA-MB-231 cells do (Fig. 1 A). Consequently, only MDA-MB-231 cells degrade gelatin in the in situ zymography assay. However, when seeded on collagen I fibrils, both cell types were able to form linear invadosomes (Fig. 1, B–D). These dynamic structures formed along collagen fibrils are composed of F-actin, cortactin, and Tks5, which are classical markers for invadosomes (Fig. 1, B and C; and Video 1). These results confirm our previous data demonstrating that type I collagen fibrils reorganized invadopodia from MDA-MB-231 cells into linear invadosomes (Juin et al., 2012). In addition, we show that type I collagen fibrils strongly induced linear invadosomes in cancer cells that do not exhibit constitutive invadopodia (Fig. 1 D). In MDA-MB-231 cells, the invadosome reorganization was also associated with an increase in the percentage of cells exhibiting these structures (Fig. 1 D) and was correlated with an increase in the global degradation activity of cells (Fig. S1 A). Altogether, we show that cancer cells expressing DDR1 can form linear invadosomes when plated on type I collagen fibrils and that contact with type I collagen fibrils increases the ability of the cells to degrade the ECM.

To investigate whether DDR1 played a role in linear invadosome formation, we analyzed DDR1 subcellular localization when cells were plated onto type I collagen fibrils. In order to do this, we transfected or infected MDA-MB-231 cells with either a DDR1-Flag construct or a DDR1-GFP lentiviral construct. We found that tagged DDR1 colocalized with linear invadosomes and type I collagen fibrils in MDA-MB-231 cells (Fig. 2 A). This result was confirmed with endogenous DDR1 when using an anti-DDR1 antibody in MDA-MB-231 and A549 cells (Fig. S1, B and C).

To determine DDR1 involvement in linear invadosome formation, we used an RNA interference strategy. Two to three distinct siRNAs were used to deplete DDR1 in both cell types (Fig. 2, B and C; and Fig. S2, A–C), and linear invadosomes were quantified upon plating on type I collagen fibrils. We found that depletion of DDR1 promoted a significant decrease in the percentage of cells able to form linear invadosomes in both cell types (Fig. 2, C and D; and Fig. S2, B and C). It also strongly decreased the number of linear invadosomes per cell (Fig. 2 E), altogether highlighting a major role of DDR1 in linear invadosome formation. To confirm these data, we performed a rescue experiment. We found that lentiviral-mediated expression of DDR1-GFP restored linear invadosome formation in cells transfected with a DDR1 siRNA, which is associated with a colocalization between Tks5 and DDR1 (Fig. S2, D and E). We have previously shown that

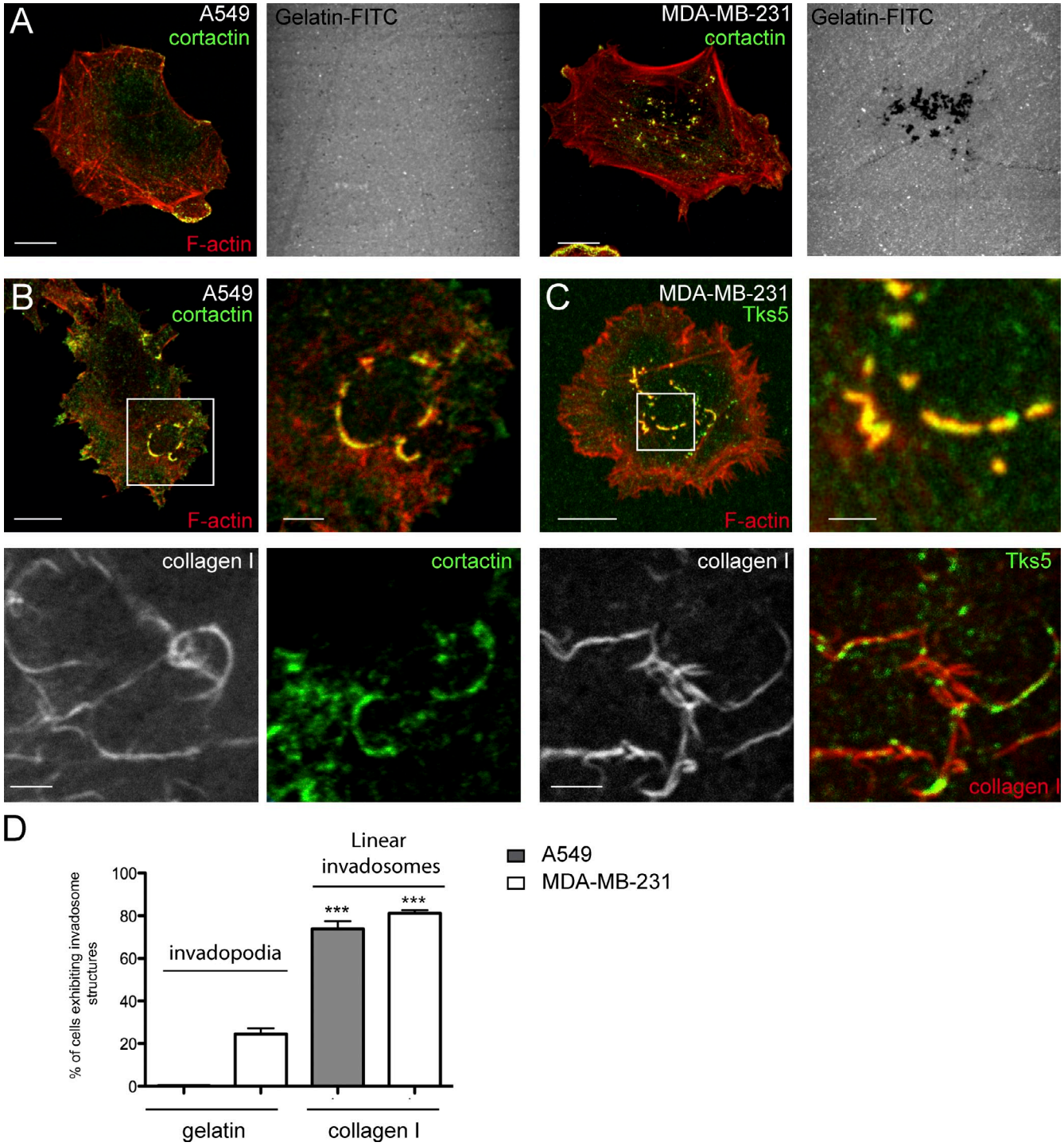

Figure 1. **DDR1-expressing cells form linear invadosomes.** (A) A549 (left) and MDA-MB-231 cells (right) were cultured on FITC-gelatin for 24 h. F-actin (red), cortactin (green), and degradation area (black) are shown. (B) A549 cells were seeded for 4 h on collagen I. (B, top) Colocalization of cortactin (green) and F-actin (red) at linear invadosomes. (B, bottom) Confocal images of linear invadosomes (cortactin, green) along collagen I fibrils (gray). (C) The same process was applied on MDA-MB-231 cells. (C, top) Colocalization of Tks5 (green) and F-actin (red) at linear invadosomes. (C, bottom) Confocal images of linear invadosomes (Tks5, green) along collagen I fibrils (gray and red in merge panel). Correlation coefficient of colocalization (collagen I/cortactin r = 0.15; collagen I/Tks5 r = 0.28; actin/cortactin r = 0.30; actin/Tks5 r = 0.23; *n* = 10). (D) Quantification of the percentage of A549 and MDA-MB-231 cells exhibiting invadopodia on gelatin versus linear invadosomes on collagen I. Values are expressed as the mean ± SEM of three independent experiments. ***, P < 0.001 as compared with plating on gelatin. Bars: (A) 5 µm; (B and C, top left) 10 µm; (B, enlarged panel on the top right) 3 µm; (B, bottom; and C, top right and bottom) 2 µm.

collagen I–induced linear invadosomes were able to degrade not only gelatin but also collagen I fibrils themselves (Juin et al., 2012). Using second harmonic generation (SHG) microscopy that allows collagen fibril visualization without any staining, we thus quantified the consequences of DDR1 depletion on collagen fibril degradation (Gailhouste et al., 2010). As

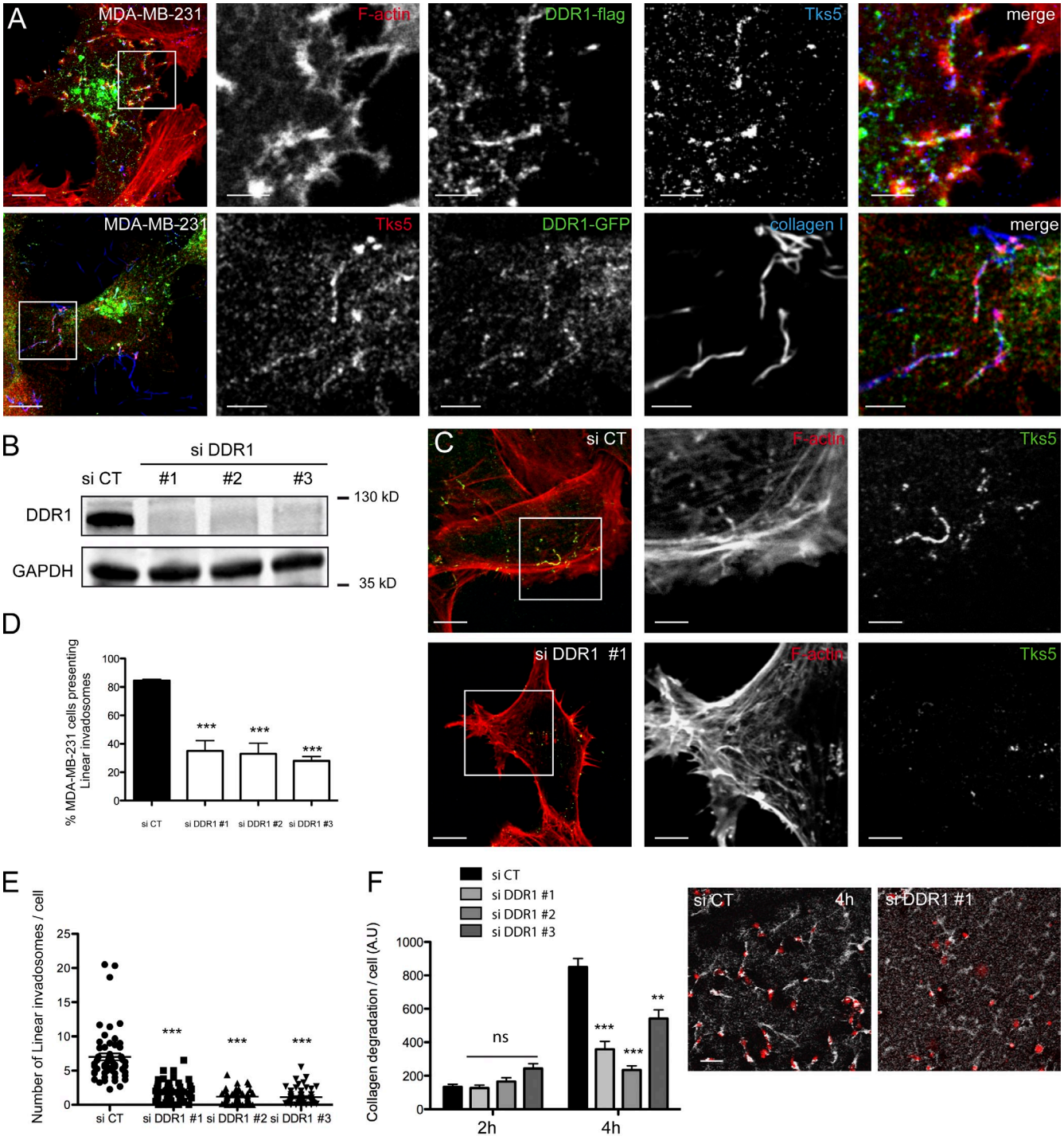

Figure 2. **DDR1 localizes at linear invadosomes and is required for their formation.** (A, top) MDA-MB-231 cells transiently transfected with DDR1-Flag were cultured for 4 h on collagen I. All channels of the boxed region are shown magnified on the right. F-actin (red) colocalizes with DDR1 (green) and Tks5 (blue) at linear invadosomes. (A, bottom) MDA-MB-231 cells stably expressing DDR1-GFP were cultured for 4 h on collagen I fibrils. Tks5 (red) colocalizes with DDR1 (green) and collagen I (blue). Correlation coefficient of colocalization: actin/DDR1 r = 0.29; DDR1/Tks5 r = 0.11; *n* = 10. (B) MDA-MB-231 cells were transfected with control (siCT) or three independent DDR1 siRNAs. DDR1 protein expression was analyzed by immunoblotting. Glyceraldehyde 3-phosphate dehydrogenase (GAPDH) was used as a loading control. (C) Cells transfected as in B were seeded for 4 h on collagen I. Shown are representative confocal images of MDA-MB-231 cells. Tks5 (green) and F-actin (red) are shown. Right panels show enlarged views of the boxed regions. Similar results were obtained with siDDR1 #2 and #3. (D–F) Down-regulation of DDR1 expression decreases the formation of linear invadosomes and their degradation activity. (D) Quantification of the percentage of MDA-MB-231 cells able to form linear invadosomes. Error bars represent the SEM (*n* > 1,000; three independent experiments; ***, P < 0.001 as compared with the control siRNA condition). (E) Quantification of the number of linear invadosomes per cell. Results are expressed as mean ± SEM (*n* > 500; three independent experiments; ***, P < 0.001 as compared with the control siRNA condition). (F) Bar graph shows the amount of collagen I degraded per cell over the time. Error bars represent the SEM (*n* = 60 fields, three independent experiments; ns, not statically significant; ***, P < 0.001; **, P < 0.005 as compared with the control siRNA condition). The right panel shows representative images of SHG collagen signals 4 h after seeding of control (siCT) or siDDR1 #1–transfected MDA-MB-231 cells. Cells are stained for Tks5 (red). Bars: (A and C, left panels) 5 µm; (A and C, magnified panels on the right) 2 µm; (E) 100 µm.

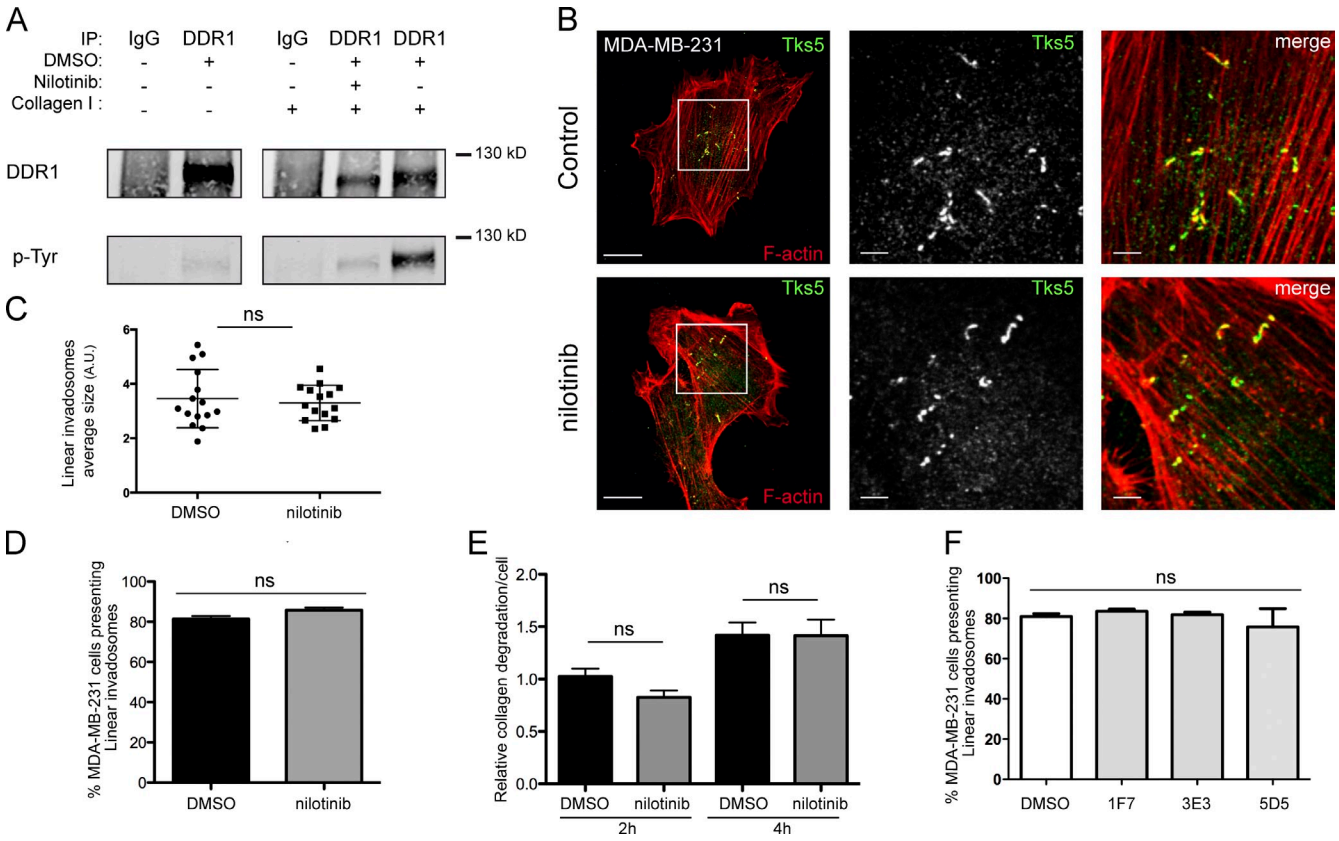

Figure 3. **DDR1 kinase activity is not necessary for linear invadosome formation and degradation activity.** (A) A549 cells were pretreated for 1 h with DMSO or 1 µM nilotinib, then seeded for 4 h on collagen I. DDR1 was immunoprecipitated and its phosphorylation assessed with a phospho-tyrosine antibody. Nilotinib treatment efficiently reduced collagen-induced DDR1 phosphorylation (representative of three experiments). (B) MDA-MB-231 cells treated with DMSO or 1 µM nilotinib were seeded on collagen I and fixed 4 h later. Shown are representative confocal images of MDA-MB-231 cells. Tks5 (green) and F-actin (red) are shown. Panels on the right show enlarged views of the boxed regions. Bars: (left) 10 µm; (magnified panels on the right) 3 µm. Correlation coefficient of colocalization: actin/Tks5 DMSO r = 0.22; nilotinib r = 0.19; n = 10. (C) The scatter plot represents the mean size of linear invadosomes in control and nilotinib conditions. n = 15 cells. There is no significant difference between the two conditions (ns, not statically significant). (D) Quantification of the percentage of cells forming linear invadosomes. Error bars represent the SEM (n > 1,000, three independent experiments). (E) Collagen degradation was monitored by SHG microscopy. The bar graph shows the amount of collagen I degraded per cell over time. Error bars represent the SEM (n = 60 fields, three independent experiments). (F) MDA-MB-231 cells were pretreated for 10 min with DMSO or the different blocking antibodies at 10 µg/ml, then cultured for 4 h on collagen I. The antibodies target the discoidin-like domain, which is outside the collagen-binding site but required for signaling. Shown is the percentage of MDA-MB-231 cells able to form linear invadosomes after treatment. Values are mean ± SEM of three independent experiments.

expected, the decrease of linear invadosome formation was correlated with a decrease in the cell capacity to degrade type I collagen fibrils (Fig. 2 F). Altogether, these results demonstrate the critical role of DDR1 in the formation and activity of type I collagen-induced invadosomes.

These results raised the question about a potential role of DDR1 in the formation and function of classical invadosomes. We thus silenced DDR1 in MDA-MB-231 and Huh6 cells, which both exhibit constitutive invadopodia. Interestingly, whereas we were not able to localize DDR1 at invadopodia, we found that decreasing DDR1 expression using two different siRNAs altered invadosome formation and decreased cell degradation capacity in MDA-MB-231 and Huh6 cells (Fig. S3).

DDR1 kinase activity is not required for linear invadosome formation and activity

As DDR1 is a tyrosine kinase receptor, we investigated the involvement of DDR1 kinase activity in linear invadosome formation and degradation function. To this end, we used nilotinib, developed as a Bcr-Abl kinase inhibitor but later shown to inhibit DDR1 kinase activity highly efficiently (Day et al., 2008). We first confirmed using immunoprecipitation that type I collagen promoted DDR1 tyrosine phosphorylation and that nilotinib almost completely abrogated it (Fig. 3 A). We found however that nilotinib treatment did not affect linear invadosome formation (Fig. 3, B–D). Indeed, type I collagen stimulation was still able to reorganize F-actin along fibrils, and Tks5 remained associated with the structures (Fig. 3 B). As assessed by the quantification of the SHG (Fig. 3 E) or of the cleaved collagen antibody signal (Fig. S4), we also found that nilotinib treatment did not affect linear invadosome degradation activity.

Moreover, we used three independent monoclonal antibodies that block DDR1 autophosphorylation without interfering with collagen binding (Carafoli et al., 2012), and we obtained the same results (Fig. 3 F), demonstrating that linear invadosome formation and activity are indeed independent of DDR1 kinase activity. In the next part of this study, we thus aimed at understanding which signaling pathway is responsible for the role of DDR1 in linear invadosome formation.

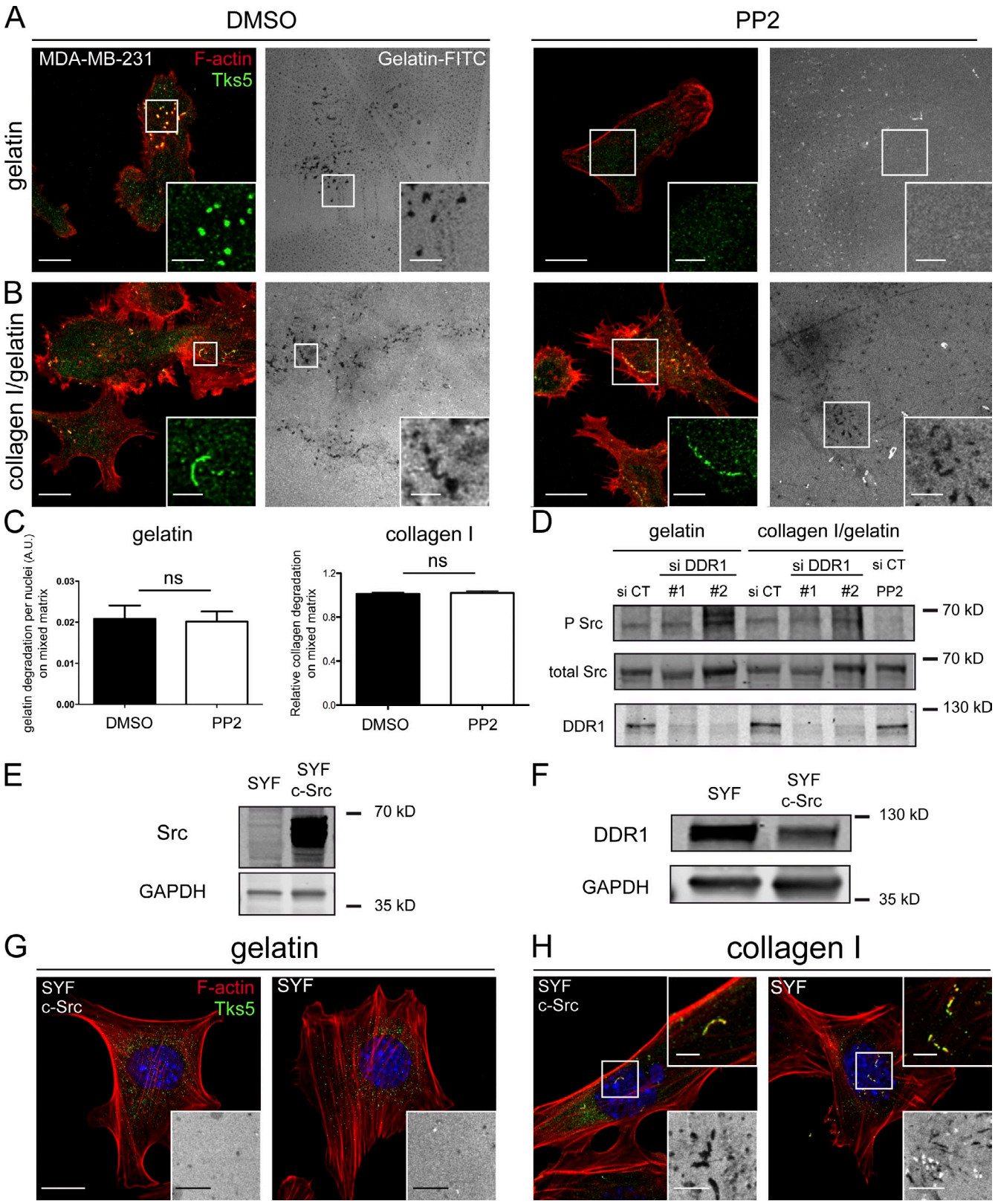

Figure 4. **Linear invadosome formation and activity is independent of Src activity.** (A and B) MDA-MB-231 cells were seeded on gelatin-FITC (top) or on a mixed matrix (collagen I/gelatin-FITC; bottom) and treated with 5 µM PP2 (Src inhibitor) or DMSO (vehicle). Gelatin (gray), Tks5 (green), and F-actin (red) are shown. (C) Quantification of the degradation capacity of MDA-MB-231 cells seeded on a mixed gelatin/collagen I matrix treated or not treated with PP2. The left graph represents the gelatin area degraded per cell after 24 h. The right graph represents the amount of collagen degraded after 4 h (n = 30 fields). Data are shown as mean ± SEM of three independent experiments. (D) MDA-MB-231 cells transfected with control (siCT) or two independent DDR1 siRNAs (DDR1 #1 and #2) were seeded on gelatin or collagen I and treated with PP2. Protein extracts were then analyzed by immunoblotting to determine phospho-Src, total Src, and DDR1 protein expression (representative of three experiments). (E and F) Western blots performed on SYF and SYF c-Src protein

c-Src is not involved in linear invadosome formation and activity

c-Src is well known as a key molecule implicated in the formation and activity of classical invadosomes (Tarone et al., 1985). Src inhibition or depletion is sufficient to abolish classical invadosome formation. In addition, c-Src has been shown to be required in DDR signaling for full phosphorylation after ligand binding (Dejmek et al., 2003; Yang et al., 2005). This prompted us to examine c-Src involvement in DDR1-induced linear invadosome formation. As expected, the c-Src inhibitor PP2 abolished invadopodia formation and degradation activity in MDA-MB-231 cells plated on gelatin (Fig. 4 A). Surprisingly, when MDA-MB-231 cells were seeded on type I collagen, or on a mixed matrix composed of gelatin associated with type I collagen fibrils, PP2 treatment had no impact on linear invadosome formation, on gelatin degradation (Fig. 4, B and C), or on type I collagen fibril degradation (Fig. 4 C). This latter finding is supported by the fact that the cleaved collagen signal was not modified upon PP2 treatment when compared with the control condition (Fig. S4).

Moreover, we demonstrated that DDR1 depletion did not modify c-Src phosphorylation whether cells were plated on gelatin or collagen I (Fig. 4 D). The lack of involvement of c-Src was confirmed using SYF cells, which do not express either Src, Yes, or Fyn, three members of the Src kinase family; and, as control, SYF-Src cells, which are the same cells that stably express c-Src (Fig. 4 E). We first confirmed that both cell lines express DDR1 (Fig. 4 F). We found that control and SYF cells do not exhibit invadopodia on gelatin (Fig. 4 G). However, when plated on a mixed matrix, SYF cells had the same potential as control cells to form linear invadosomes, and these invadosomes were fully active at degrading the matrix (Fig. 4 H). All these results show that c-Src is not involved in the formation or in the degradation activity of type I collagen–induced linear invadosomes.

Cdc42 is the main RhoGTPase involved in the formation of linear invadosomes

It is well established that RhoGTPases, principally RhoA, Rac1, and Cdc42, control actin cytoskeleton remodeling and invadosome formation (Linder et al., 2011). Using siRNAs targeting these three proteins, we investigated their respective involvement in linear invadosome formation. We used two distinct siRNAs per GTPase and first checked their efficiency by specifically depleting their corresponding targets (Fig. 5 A). We then measured their impact on linear invadosome formation. We found that only Cdc42 depletion had an impact on linear invadosome formation (Fig. 5, B and C). We then expressed constitutively active and inactive forms of Cdc42 in MDA-MB-231 cells seeded on type I collagen fibrils. We found that the constitutively active form of Cdc42, GFP-V12Cdc42, colocalized with linear invadosomes (Fig. 6 A), unlike the Cdc42 dominant-negative form, GFP-N17Cdc42 (Fig. 6 B). Moreover, we found that expression of GFP-V12Cdc42 enhanced the ability of MDA-MB-231 cells to form linear invadosomes, whereas expression of GFP-N17Cdc42 had the opposite effect (Fig. 6 C). It has been shown that type I collagen fibrils can promote Cdc42 activation (Sato et al., 2003). We thus analyzed the activity level of Cdc42 in cells plated on type I collagen fibrils with or without depletion of DDR1. We first confirmed that type I collagen significantly promoted Cdc42 activation, and found that this effect of type I collagen was abolished in cells with DDR1 depletion (Fig. 6 D). This result was strengthened by the colocalization of DDR1 with the active form of Cdc42 (Fig. 6 E). In addition, using the Raichu Cdc42 biosensor (Itoh et al., 2002) on living cells seeded on type I collagen, we showed a signal corresponding to activated Cdc42 along collagen fibrils (69 hits with a high FRET ratio along collagen fibrils out of 79 cells observed; Fig. 6 F). All these data show that Cdc42 is involved in relaying the collagen I signal through DDR1 for the formation of linear invadosomes.

Tuba, a Cdc42-specific guanine nucleotide-exchange factor (GEF), is required for linear invadosome formation

To go further concerning the link between DDR1 and Cdc42, we searched for a GEF involved in Cdc42 activation upon type I collagen fibril induction. For this purpose, we performed an RNAi screen targeting 14 Cdc42-specific GEFs (Table S1) on cell ability to form linear invadosomes (Cook et al., 2014). Our screen revealed that the depletion of the GEF Tuba impacts on linear invadosome formation. Tuba is a Cdc42-specific GEF but also acts as a scaffold protein to link dynamin with actin regulatory proteins such as N-WASP. To confirm this result, we used two distinct siRNAs to deplete Tuba expression in MDA-MB-231 and A549 cells (Fig. 7, A and B). We demonstrated that Tuba depletion induces a decrease in cell ability to form linear invadosomes in both cell types (Fig. 7, A–C). In addition, we observed a colocalization between DDR1 and Tuba in linear invadosomes of DDR1-GFP–expressing cells that supports a link between these two molecules (Fig. 7 D). Thus, this is the first demonstration of the involvement of Tuba in invadosome formation. To address Tuba participation in classical invadopodia, we analyzed Tuba localization in MDA-MB-231 cells seeded on gelatin. Interestingly, Tuba did not colocalize with classical invadosomes while it was present on linear invadosomes (Fig. 7 E). These data suggest that DDR1 can recruit Tuba that can specifically activate Cdc42 to induce linear invadosome formation.

DDR1 depletion decreases cancer cell invasion capacities

DDR1 is known to be involved in cancer cell invasion and metastasis induction (Valiathan et al., 2012). Because type I collagen fibrils are part of the tumor microenvironment, we studied

extracts representing, respectively, protein expression of Src and DDR1. GAPDH was used as a loading control. (G and H) Confocal images of control cells (SYF c-Src) and SYF fibroblasts cultured on gelatin (G) or on a mixed matrix (gelatin/collagen I; H) for 24 h and processed for immunofluorescence staining (F-actin, red; Tks5, green; DAPI, blue). Insets on the bottom show gelatin-degraded pictures. Bars: (A, G, and H) 10 µm; (A, insets) 7 µm; (H, top insets) 2 µm; (G and H, bottom insets) 10 µm.

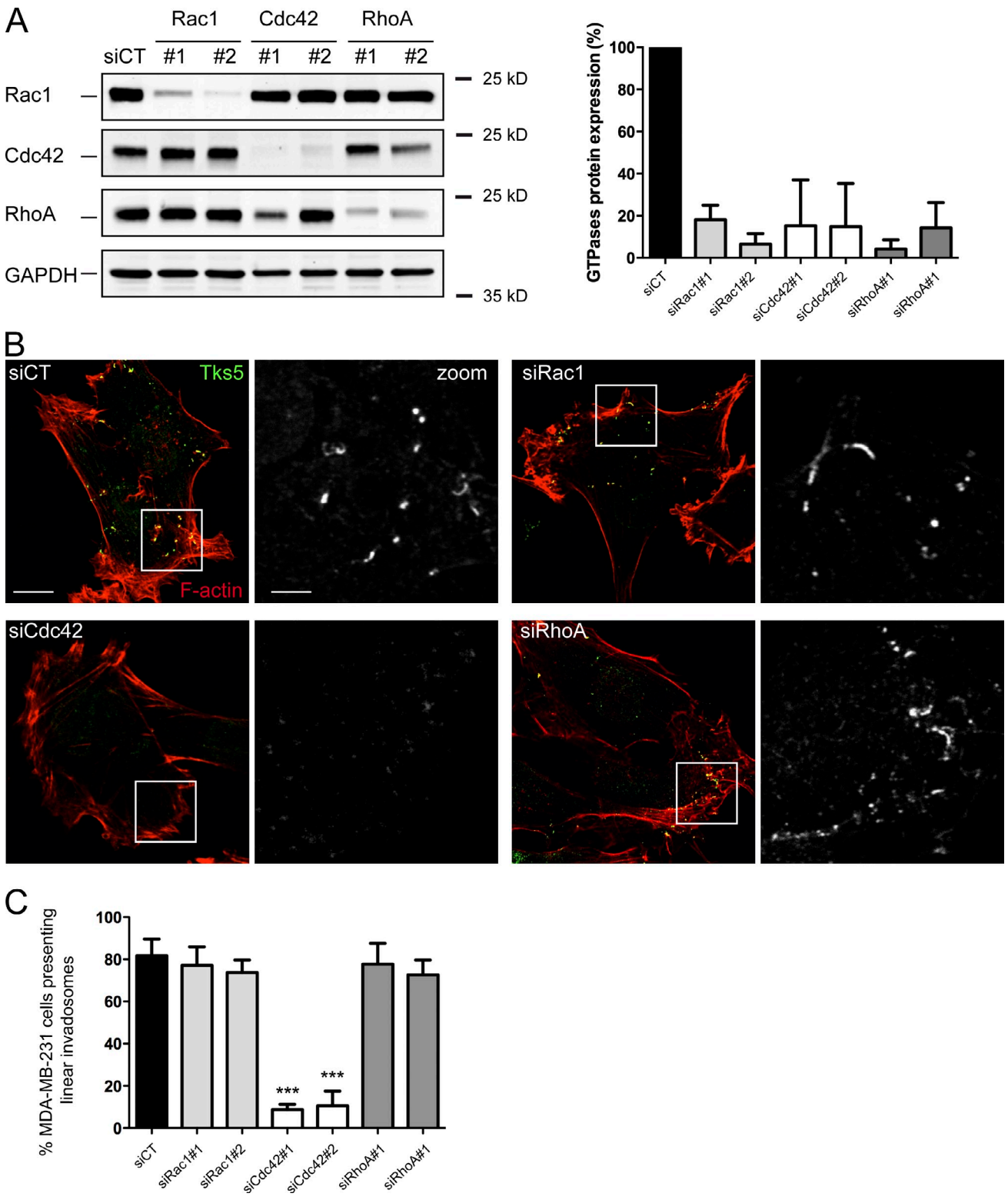

Figure 5. **Cdc42 drives linear invadosome formation via DDR1.** (A) Western blot analysis of MDA-MB-231 cells transfected with siRNA control (siCT) or two independent siRNAs targeting Rac1, Cdc42, or RhoA. GAPDH is used as a loading control. Three independent experiments were realized and quantified to demonstrate a specific effect on targeted RhoGTPase expression represented on the bar graph on the right. (B and C) MDA-MB-231 cells transfected as in A were cultured on collagen I for 4 h, fixed, and processed for immunofluorescence staining. (B) Representative confocal images of MDA-MB-231 cells transfected as in A. Tks5 (green) and F-actin (red) are shown. Panels on the right show enlarged views of the boxed regions. Bars: (left) 10 µm; (enlarged panels on the right) 2.5 µm. (C) The percentage of siRNA-transfected MDA-MB-231 cells able to form linear invadosomes was quantified. Error bars represent the SEM (n > 1,000, three independent experiments; ***, $P < 0.001$ as compared with the control siRNA condition [siCT]).

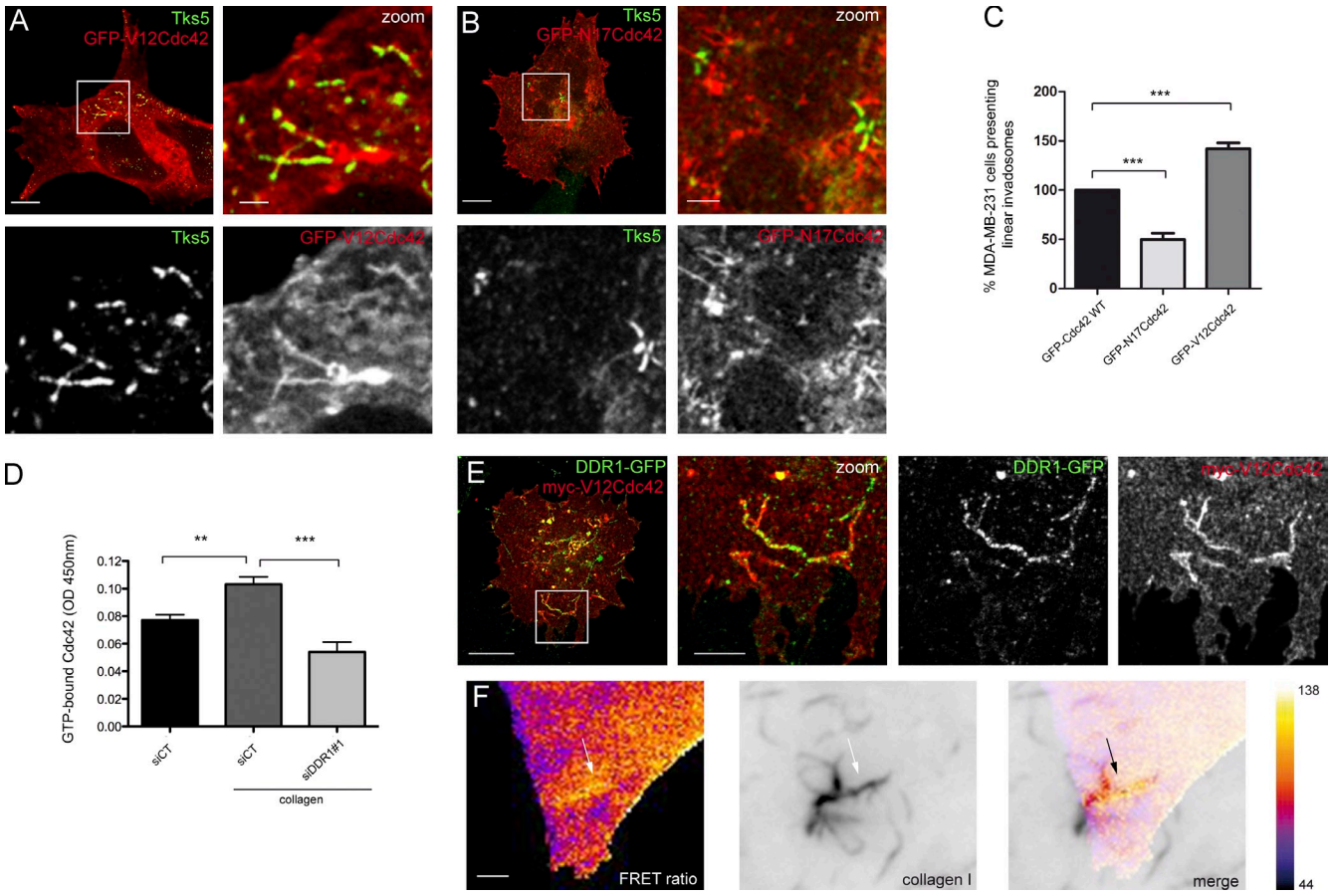

Figure 6. **Activated Cdc42 colocalizes with linear invadosomes, DDR1, and collagen I fibrils.** (A and B) MDA-MB-231 cells transiently transfected with GFP-V12Cdc42 or GFP-N17Cdc42 were cultured for 4 h on collagen I. Tks5 (green) colocalizes with GFP-V12Cdc42 (red) at linear invadosomes whereas GFP-N17Cdc42 (red) does not. Panels on the right show enlarged views of the boxed regions. Correlation coefficient of colocalization: Tks5/V12Cdc42 r = 0.21; Tks5/N17Cdc42 r = −0.11 (n = 25). (C) Quantification of the percentage of GFP-WTCdc42–, GFP-V12Cdc42–, and GFP-N17Cdc42–transfected cells able to form linear invadosomes. Data are mean ± SEM (n > 500, three independent experiments; ***, P < 0.001). (D) Active Cdc42 level was monitored in MDA-MB-231 cells treated as indicated. Data are mean ± SEM, three independent experiments. **, P < 0.005; ***, P < 0.001. (E) MDA-MB-231 stably expressing DDR1-GFP transiently transfected with myc-V12Cdc42 were seeded for 4 h on collagen I (DDR1-GFP, green; myc-V12Cdc42, red). Panels on the right show an enlarged view of the boxed region. Correlation coefficient of colocalization: DDR1/mycV12Cdc42 r = 0.15 (n = 10). (F) MDA-MB-231 cells were transfected with Raichu-Cdc42 and seeded on labeled collagen I. Shown are representative images: on the left, the pseudocolored ratio image generated from YFP/CFP ratio images represents the FRET ratio, which correlates with the Cdc42 activity (in yellow); and on the right, a collagen I image. Arrows represent colocalization of active probe and collagen I fibrils. Bars: (A and B, left) 5 µm; (A and B, right) 2.5 µm; (E, left) 7 µm; (E, enlarged panels on the right) 2 µm; (F) 3 µm.

whether DDR1 was involved in the invasion of a 3D collagen gel by linear invadosome-bearing tumor cells. We first demonstrated that MDA-MB-231 cells were able to form linear invadosomes in a 3D collagen gel (Fig. 8 A). We further used an invasion assay (Lopez et al., 2005) consisting of a type I collagen gel polymerized into Boyden chambers. Gels were polymerized at a 1 mg/ml concentration of type I collagen at 37°C for 1 h. In this condition, cells need proteolysis to invade the gel according to the study of Wolf et al. (2013). Cells were seeded on top of the collagen gel and fixed after 1 h and 3 d. We confirmed that DDR1 depletion remained constant over the studied time frame (Fig. 8 B). Using quantitative confocal z-stack analysis (Fig. 8 C), we found that DDR1 depletion blocked the cell's ability to invade the collagen gel. In the control condition, approximately half of the cells were able to invade the gel (Fig. 8 D). In contrast, DDR1 down-regulation abolished cell invasion. Confocal analysis showed that after 3 d, most of the DDR1-silenced cells remained stacked at the gel surface and did not enter into the gel (Fig. 8 E). To control that cells used a proteolysis-dependent mode of migration to invade the collagen gel, we used an MMP inhibitor, GM6001. We found that GM6001 totally blocked the cell's ability to penetrate the gel, demonstrating the MMP involvement in this process (Fig. S5, A and B). Consequently, GM6001 treatment abolished the cleaved collagen signal observed in the control condition (Fig. S5 C). As PP2 and nilotinib treatments did not inhibit type I collagen degradation in 2D (Fig. S4), we also checked for cell invasion in 3D in these conditions. PP2 treatment did not have an impact on cell invasion, whereas nilotinib treatment only induced a slight decrease in the cell capacity to invade the collagen gel (Fig. S5, A and B). These data demonstrate the crucial involvement of DDR1 in type I collagen matrix invasion, which we found to be MMP dependent and Src independent.

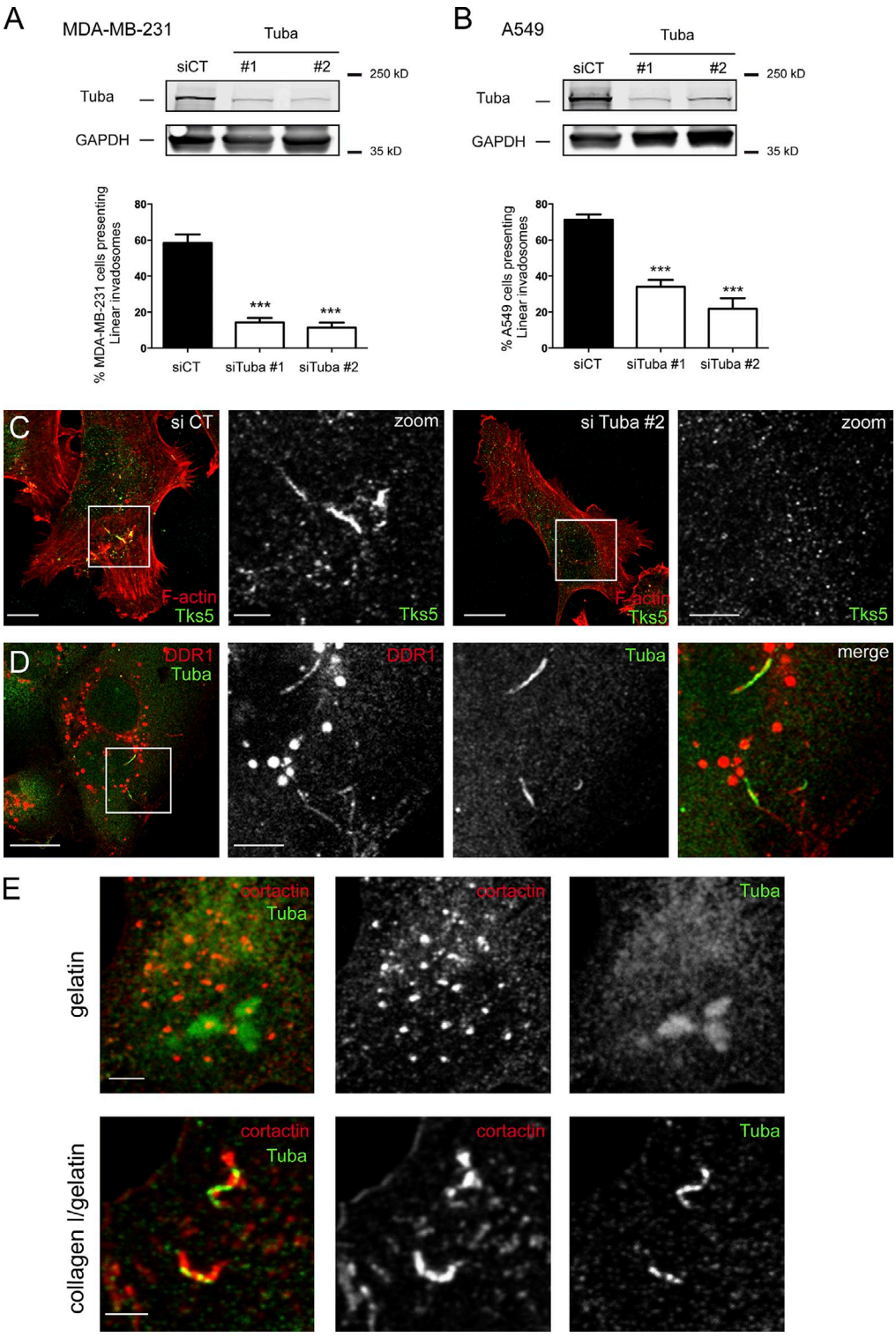

Figure 7. **The GEF Tuba is specifically implicated in linear invadosome formation.** (A and B) From left to right, MDA-MB-231 and A549 cells were transfected with control (siCT) or two independent Tuba siRNAs (Tuba #1 and #2). Tuba protein expression was analyzed by immunoblotting. GAPDH was used as a loading control. The graphs show quantification of the percentage of cells able to form linear invadosomes. Error bars represent the SEM (n = 900, three independent experiments; ***, $P < 0.001$ as compared with the control siRNA condition). (C) MDA-MB-231 cells were treated as in A and seeded for 4 h on collagen I. Shown are representative confocal images of MDA-MB-231 cells. Tks5 (green) and F-actin (red) are shown. Panels on the right show enlarged views of the boxed regions. Similar results were obtained with siTuba #2. Tuba extinction decreases the capacity of cells to form linear invadosomes. (D) MDA-MB-231 cells stably expressing DDR1-GFP were seeded for 4 h on collagen I and fixed. Immunofluorescence with endogenous Tuba (green) and DDR1-GFP (red) was performed and reveals a colocalization of the GEF Tuba with DDR1. Right panels show enlarged views of the boxed region. Correlation coefficient of colocalization: DDR1/Tuba r = 0.15 (n = 10). (E) MDA-MB-231 cells were seeded on gelatin (top) or mixed matrix (collagen I/gelatin) for 24 h and 4 h, respectively, then processed for immunofluorescence staining (cortactin, red; Tuba, green). While Tuba is not present on classical invadosomes, it colocalizes with cortactin on linear invadosomes. Bars: (C, left) 5 µm; (C, enlarged panels on the right) 2 µm; (D, left) 10 µm; (D, enlarged panels on the right) 3 µm; (E) 3 µm.

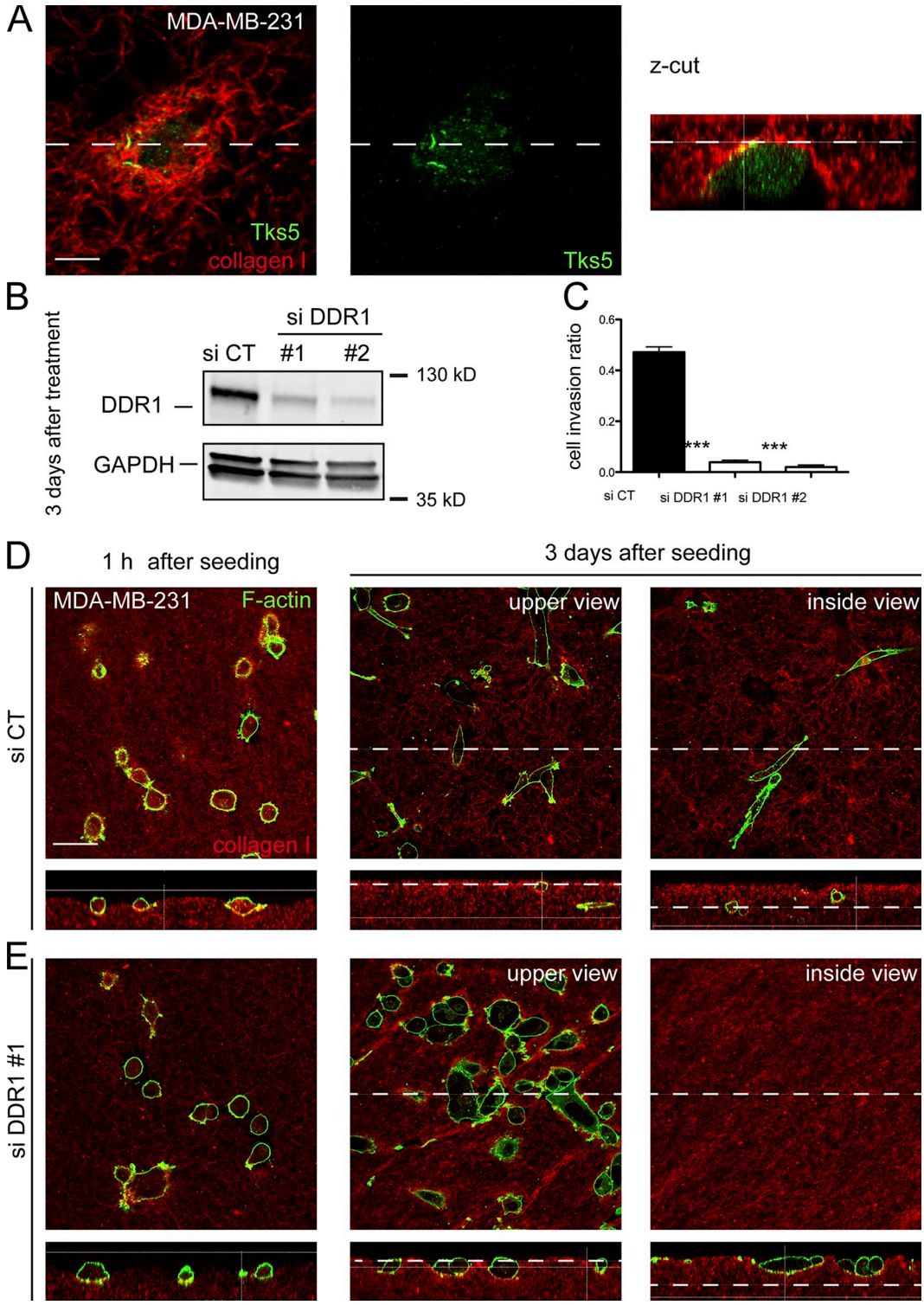

Figure 8. **DDR1 is required for invasion of invadosome-bearing cells in 3D collagen matrix.** (A) MDA-MB-231 cells were placed for 4 h into a 3D collagen gel (red), fixed, and processed for immunofluorescence staining (Tks5, green). The z-cut section is shown on the right. The broken line on the left panel corresponds to the focal plane shown in the z-cut section. (B) DDR1 expression in MDA-MB-231 cells transfected with control siRNA (siCT) or two siRNAs targeting DDR1 (siDDR1 #1 and #2) was monitored 3 d after cell seeding (anti-DDR1 [D1G6]; Cell Signaling Technology). (C–E) MDA-MB-231 cells transfected as in B were seeded for an invasion assay and allowed to invade the collagen matrix for 1 h or 3 d. Z confocal optical sections were taken. (C) Assays were quantified by measuring an invasion index. The bar graph represents the ratio of the number of MDA-MB-231 cells penetrating the collagen gel/number of seeded cells. Data are expressed as mean ± SEM (three independent experiments). ***, $P < 0.001$ as compared with control siRNA (siCT). (D and E) Representative confocal images of MDA-MB-231 cells transfected with control siRNA (siCT) or siRNA targeting DDR1 seeded on collagen I fibrils. F-actin, green; collagen I fibrils, red. Images were taken 1 h (left) or 3 d after seeding (middle and right). Top panels correspond to focal planes whereas bottom panels represent matched z-cut sections. The broken lines on the bottom panel correspond to focal planes. 1 h after seeding, MDA-MB-231 cells transfected with control or siDDR1 #1 are on the top of the gel. 3 d later, control MDA-MB-231 cells deeply invaded the collagen plug (D, right), whereas DDR1-depleted cells were still on the top of the collagen plug (E, right). Bars: (A) 5 µm; (D and E) 50 µm.

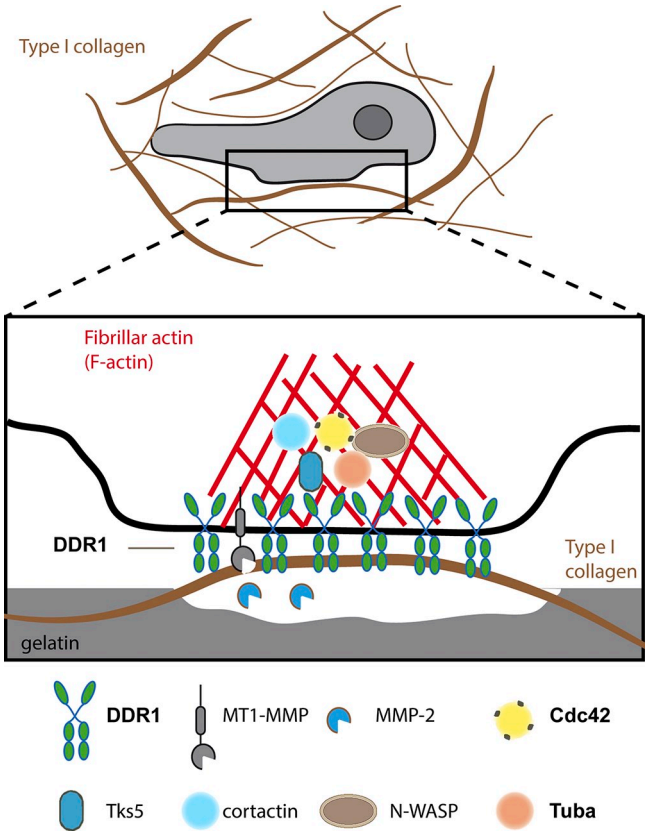

Figure 9. **DDR1 controls linear invadosome formation via Tuba-dependent Cdc42 activation.** Schematic representation of linear invadosome architecture and molecular composition. When cells are seeded on fibrillar type I collagen, DDR1 is activated along the fibrils, leading to the activation of Cdc42 via Tuba GEF and recruiting classical components of invadopodia such as N-WASP, cortactin, and scaffold protein Tks5 to form linear invadosomes. Linear invadosomes are able to degrade extracellular matrix elements via MT1-MMP and MMP2 (Juin et al., 2012).

Discussion

This study has revealed the link between the collagen receptor DDR1 associated with the development of metastasis, and invadosomes, which are protrusive F-actin structures used by tumor cells to degrade the ECM and promote invasion. Herein, we confirmed our previous findings showing the importance of type I collagen fibrils as powerful invadosome inducers (Juin et al., 2012) and extend them to cancer cells. Most cell types are able to form linear invadosomes, including endothelial cells, fibroblasts, cancer cells, Src-transformed cells (Juin et al., 2012), or, as shown by another group, megakaryocytes (Schachtner et al., 2013). We demonstrated that the simple contact of cancer cells with type I collagen fibrils can promote formation of linear invadosomes and consequently activate their capacity to degrade the ECM. In the case of cancer cells constitutively exhibiting invadopodia, type I collagen fibrils induced their reorganization into linear invadosomes, increased the percentage of cells presenting linear invadosomes as compared with classical invadopodia, and also increased the capacity of the cells to degrade the ECM. Owing to their capacity to localize the degradation machinery along fibrils, linear invadosomes could be implicated in the proteolytic breakdown of the ECM, which favors invasive migration, either in physiological conditions such as angiogenesis, or in pathological situations such as cancer. Thus, there is a great interest in developing our understanding of the molecular pathways required for the formation and function of linear invadosomes.

Although integrins are required for the formation and activity of classical invadosomes (Destaing et al., 2010; Beaty et al., 2013), we found that they are not necessary for linear invadosome formation (Juin et al., 2012), thus raising the question of the identity of the collagen receptor responsible for their formation. Four major classes of vertebrate transmembrane receptors are known to interact directly with the native collagen triple helix: collagen-binding β1 integrins, DDRs, glycoprotein VI (GPVI), and leukocyte-associated immunoglobulin-like receptor-1 (LAIR-1; Hidalgo-Carcedo et al., 2011; Leitinger, 2011). Our own data eliminated β1 integrins (Juin et al., 2012). Because GPVI is present only on platelets and LAIR-1 on leukocytes, we turned our attention to the DDRs, which are ubiquitously expressed.

We found that DDR1 colocalized within linear invadosomes, and, using a RNAi approach, found that it was involved in their formation and in their ability to degrade type I collagen fibrils. These results establish DDR1 as the collagen I receptor required for linear invadosome formation (Fig. 9) and raise the question of DDR1's role in classical invadosomes. We showed that DDR1 depletion decreased classical invadosome formation and activity. Importantly, the effect of DDR1 on classical invadosomes was observed on gelatin, which is not known as a DDR1 substrate. Accordingly, we were unable to colocalize DDR1 with classical invadosomes. However, these data suggest an involvement of DDR1 in classical invadopodia. Because DDR1 controls integrin activation (Xu et al., 2012), it could modulate invadosome formation and activation directly or indirectly. Moreover, DDR1 and integrins present common signaling pathways, which suggests a cooperative action to form classical invadosomes (Shintani et al., 2008).

Because DDR1 is an RTK, we investigated the role of its kinase activity in invadosome formation. We demonstrated, using nilotinib as an inhibitor as well as blocking antibodies, that DDR1 kinase activity is not necessary for the formation of linear invadosomes. This is in agreement with our previous observations. Indeed, we found that linear invadosomes already appear within 10 min of cell seeding on type I collagen, a kinetic that is not compatible with DDR autophosphorylation, a slow process requiring >30 min before being detectable (Shrivastava et al., 1997; Vogel et al., 1997; Juin et al., 2012). Interestingly, it was previously shown that the role of DDR1 in promoting collective migration was also independent of its kinase activity (Hidalgo-Carcedo et al., 2011). In our hands, the lack of requirement for c-Src activity, demonstrated with both a pharmacological antagonist and the use of SYF cells, is also in line with these findings because it was shown that c-Src was necessary for the full DDR phosphorylation (Dejmek et al., 2003; Yang et al., 2005). In addition, although c-Src has been historically associated with invadosomes, our data show that collagen I–induced invadosomes are independent of c-Src

activity. Thus, linear invadosomes are the first described c-Src kinase–independent invadosomes.

How then does DDR1 signal for invadosome formation? As the RhoGTPases RhoA, Rac1, and Cdc42 have been largely involved in invadosome formation and organization, we investigated their role in DDR1-dependent linear invadosome formation. We clearly showed that only Cdc42 is involved. This is supported by the drastic effect of Cdc42 silencing, the blockage of collagen I–induced Cdc42 activation in cells transfected with DDR1 siRNAs, and the localization of the active form of Cdc42 (GFP-V12Cdc42 protein and Cdc42 biosensor) at linear invadosomes. Conversely, the GFP-N17Cdc42 dominant-negative form decreased the cell's ability to form linear invadosomes on collagen and did not colocalize with linear invadosomes. Most invadosome models are controlled and regulated by several Rho-GTPases. Our results are thus important, as only very few models have been described so far in which only Cdc42 and not RhoA or Rac1 are implicated in invadosome formation. This specificity of linear invadosomes, together with their restricted molecular composition, which we reported previously (Juin et al., 2012), supports the idea that collagen-induced invadosomes correspond to a minimal form of invadosomes (Di Martino et al., 2014). Intriguingly, another study showed that overexpression of tagged forms of DDR1 in MDCK cells decreased Cdc42 activation by collagen (Yeh et al., 2009). The reason for this discrepancy is unclear, but it may be relevant to explain why MDCK cells are unable to form linear invadosomes and to degrade the ECM upon collagen stimulation (unpublished data).

Altogether, our data demonstrated that collagen I–induced invadosomes rely on a DDR1, Cdc42-dependent pathway (Fig. 9). We further identified Tuba as the major Cdc42GEF involved in linear invadosome formation. Several other Cdc42GEFs such as FGD1 or Vav1 were shown to be involved in invadopodia formation (Ayala et al., 2009; Razidlo et al., 2014), but this is the first demonstration of the involvement of Tuba. Moreover, Tuba colocalized with DDR1 into linear invadosomes but not with classical invadosomes, which allowed us to identify Tuba in addition to DDR1 as a specific marker of linear invadosomes. Tuba is a 177-kD protein containing four SH3 domains in its N terminus: a central GEF domain, followed by a BAR domain and two SH3 domains in the C terminus (Cestra et al., 2005; Xu et al., 2012). The involvement of Tuba is in line with the involvement of N-WASP in linear invadosomes, as Tuba was shown to be involved in N-WASP–dependent cytoskeletal rearrangements (Salazar et al., 2003; Kovacs et al., 2006). Though we describe here the involvement of Tuba in MDA-MB-231 and in A549 cells, it is now clear that each cancer cell expresses its own pattern of GEFs among the 70 RhoGEFs in the human genome, (Cook et al., 2014; Razidlo et al., 2014), which suggests that other GEFs may also be involved in linear invadosome formation according to the cell type. In addition, the link between DDR1 and Tuba is probably not direct, as we were not able to show an interaction between both proteins. Indeed, other DDR1-interacting proteins could also be involved. For instance, on one hand several studies have identified DDR1 partners previously linked to the invadosome machinery (Murphy and Courtneidge, 2011), like PYK2 (Shintani et al., 2008), Nck2 (Koo et al., 2006), and PI3K (Dejmek et al., 2003), whereas others found DDR1-interacting partners that bind DDR1 regardless of its phosphorylation status, like Syk (Dejmek et al., 2005), E-cadherin (Hidalgo-Carcedo et al., 2011), and the Par3/Par6 cell polarity proteins (Hidalgo-Carcedo et al., 2011). Further studies will tell if these proteins are involved in the role of DDR1 on linear invadosome formation and activation.

In our study, we confirmed the role of DDR1 in cell invasion. However, interestingly, we established that inhibition of Src with PP2 or of DDR1-kinase activity with nilotinib did not affect drastically type I collagen degradation and cell invasion. This differs from the findings from other studies showing an impact of PP2 treatment on cell invasion (Angers-Loustau et al., 2004). This point could be explained by the conditions used to perform these assays such as the use of a non–type I collagen matrix, the collagen source, or the absence of serum starvation. It is clear that the kinase activity of the receptor is crucial for DDR1 signaling that promotes, for example, cell proliferation. But we demonstrated here that cells can sense type I fibrils and start a degradation process independent of its kinase activity and in the absence of a requirement for c-Src.

Thus, upon contact with type I fibers, DDR1 is able to recruit the actin machinery associated with a strong matrix degradation activity. Although the proteolytic mechanisms used by linear invadosomes are still being investigated, a recent study has shown that the Scar homologue (WASH) and the exocyst complex are involved in delivering MT1-MMP–positive late endosomes focally to linear invadosomes (Monteiro et al., 2013). It is well known that MMPs, such as pro-MMP2, can be activated by the culture of cells on fibrillar collagen I (Azzam and Thompson, 1992; Ruangpanit et al., 2001) in an MT1-MMP–dependent manner (Takino et al., 2004). Thus, we propose that DDR1 is the sensor used by tumor cells to interact with fibrillar collagen I, leading to the organization of invadosomes that concentrate the proteolytic machinery of the cells to facilitate invasiveness. Because of its capacities to stimulate cell invasion and its overexpression in different cancers, DDR1 should be a good target for the prevention of metastasis.

Materials and methods

Antibodies, reagents, and constructs

Nilotinib, anti-Tks5 (rabbit, M-300), anti-DDR1 (rabbit, C-20), anti-GAPDH (mouse, FL-335), anti-myc (mouse, 9E10), and anti-RhoA (mouse, 26C4) antibodies were purchased from Santa Cruz Biotechnology, Inc. Mouse anti-DDR1 monoclonal antibodies (1F7, 1F10, 3E3, and 5D5) were provided by B. Leitinger (National Heart and Lung Institute, Imperial College London, London, England, UK) and produced as described previously (Carafoli et al., 2012). Mouse anti–β-actin (clone AC-15), anti-tubulin (T6074), and anti-Flag (clone M2) antibodies were purchased from Sigma-Aldrich. We also used anti-DDR1 (rabbit, D1G6) from Cell Signaling Technology. Anti-cortactin (mouse, p80/85), anti-Rac1 (mouse, 23A8), anti-Src CT (rabbit, clone NL19), anti–phospho-Src (mouse, Tyr416), and anti-phosphotyrosine (mouse, 4G10) antibodies and GM6001 were purchased from EMD Millipore. Anti-Cdc42 (mouse, clone 44) antibody was purchased from BD. PP2 was from Abcam. Anti–collagen type I cleavage site antibody (rabbit, Col1 3/4 short C) was purchased from immunoGlobe. Rabbit polyclonal anti-Tuba antibody was provided by P. De Camilli (Yale University, New Haven, CT; Salazar et al., 2003; Cestra et al., 2005). Secondary antibodies FluoProbes 488, 547H, and 647H anti–rabbit and anti–mouse antibodies were purchased from Interchim. F-actin was stained with Phalloidin-FluoProbes 647, 547H, 488, or 405 (Interchim). Hoechst 34580 (Invitrogen) was used to

stain nuclei. To visualize the collagen I network, we labeled 0.4 mg/ml fibrillar collagen I with 10 µg/ml Alexa Fluor 546 or 647 carboxylic acid succinimidyl ester (Invitrogen).

pDDR1-Flag construct was provided by M. Bendeck (Laboratory Medicine and Pathobiology, University of Toronto, Toronto, Ontario, Canada). Human DDR1 full length fused to flag sequence was cloned in pcDNA3.1/Zeo (−) using EcoRI–BamHI cloning sites, placed under the control of a cytomegalovirus (CMV) promoter. pEGFP-Cdc42 WT, pEGFP-V12Cdc42, myc-V12-Cdc42, and pEGFP-N17Cdc42 have been described previously (Moreau et al., 2003). GFP-Cdc42–tagged constructs were cloned in pEGFP-C1 using BglII–KpnI cloning sites and placed under the control of a CMV promoter. pLVX-EF1α-DDR1-acGFP was constructed from pcDNA 3.1/zeo–DDR1–myc (provided by G.D. Longmore, ICCE Institute, Washington University School of Medicine, St. Louis, MO; Zhang et al., 2013) by subcloning DDR1 full length under the control of an EF1α promoter into pLVX-EF1α–acGFP-N1 (Takara Bio Inc.) using AfeI and BamHI restriction sites. pRaichu-Cdc42 was provided by M. Matsuda (Graduate School of Biostudies, Kyoto University, Kyoto, Japan; Aoki and Matsuda, 2009). pRaichu-Cdc42 was derived from the pCAGGS eukaryotic expression vector and encoded a chimeric protein, Raichu-Cdc42. pLifeact-mRuby lentiviral vector was obtained by subcloning Lifeact-mRuby from pmRFPRuby-Lifeact, provided by R. Wedlich-Soeldner (Max Planck Institute of Biochemistry, Martinsried, Germany; Riedl et al., 2010), using BglII and SpeI restriction sites in pRRLsin-MND-MCS-WPRE lentiviral plasmid, placed under the control of an MND promoter. pTks5-GFP was provided by S.A. Courtneidge (Sanford-Burnham Medical Research Institute, La Jolla, CA). Human Tks5 was cloned in pcDNA3.1/Zeo (−) using XhoI–Kpn I cloning sites, placed under the control of a CMV promoter.

Cell culture

MDA-MB-231 cells (human breast cancer cell line) were from American Type Culture Collection and were maintained in L-15 medium and Glutamax-I (Invitrogen) supplemented with 10% fetal calf serum and 100 U/ml penicillin–streptomycin (Invitrogen). A549 (human lung adenocarcinoma cell line) were from Sigma-Aldrich, provided by F. Delom (INSERM, Bordeaux, France), and SYF and SYF c-Src fibroblasts were from A. Wiedmann (INRA Val de Loire, Tours, France; Klinghoffer et al., 1999). Huh6 cells (human hepatoblastoma cell line) were provided by C. Perret (Cochin Institute, Paris, France). A549 and SYF cell lines were cultured in Dulbecco's modified Eagle's medium with 4.5 g/liter glucose Glutamax-I (Invitrogen) supplemented with 10% fetal calf serum (Pan Biotech GmbH) and 100 U/ml penicillin–streptomycin (Invitrogen). The Huh6 cell line was cultured in Dulbecco's modified Eagle's medium with 1 g/liter glucose Glutamax-I (Invitrogen) supplemented as with A549 cells.

Transfections and infections

SiRNA oligonucleotides (100 nM) were transfected with Lipofectamine RNAiMax (Invitrogen) according to the manufacturer's instructions. The siRNA sequences for human DDR1 were as follows. DDR1 #1, 5′-GAAUGUCGCUUCCGGCGUGUU-3′;DDR1#2,5′-GAGCGUCUGUCUGCGGGUAUU-3′ according to published sequences (Hidalgo-Carcedo et al., 2011). DDR1 #3 (SI05130706; QIAGEN) targets the 3′ UTR of DDR1 mRNA. The antisense strand siRNA was targeted against GTPases using the 21-nucleotide sequences 5′-AAGAAGTCAGCATTTCTGTC-3′ for hRhoA #1, 5′-AAGTTCTTAATTTGCTTTTCC-3′ for hRac1 #1, and 5′-AAGATAACTCACCACTGTCCA-3′ for hCdc42 #1 according to published sequences (Deroanne et al., 2003); 5′-AAGGAGATTGGTGCTGTAAAA-3′ for hRac1 #2 as previously published (Grise et al., 2012); and 5′-AGGTGGATGGAAAGCAGGTA-3′ for hRhoA #2 and 5′-GAGATGACCCCTCTACTATTG-3′ for hCdc42 #2. A control siRNA targeted against luciferase (CT) 5′-CGTACGCGGAATACTTCGA-3′ was purchased from Eurofins MWG Operon, Inc. siRNAs used for the GEF screen were purchased from QIAGEN and are referenced in Table S1. The second siRNA sequence for human Tuba was as follows: Tuba #2, 5′-GAGCUUGAGGGAACAUACAAGAUUU-3′, as previously published (Rajabian et al., 2009). For transient transfection of MDA-MB-231 cells, the Amaxa Nucleofector kit V (Amaxa Inc.), JET PRIME (PolyPlus; Ozyme), or Lipofectamine 2000 (Invitrogen) was used according to the manufacturer's instructions. 5 µg of DNA was added per well of a six-well plate. Cells were allowed to grow 24 h after transfection before use.

For the rescue experiment, cells were transfected with siRNA DDR1 #3 to silence endogenous DDR1 as described in the same paragraph. 2 d after, siRNA DDR1-expressing cells were infected with lentivirus particles expressing DDR1-GFP at a multiplicity of infection of 2.5 and selected using puromycin antibiotic at a concentration of 1 µg/ml. The rescue was observed comparing the proportion of cells able to form linear invadosomes in cells receiving siRNA control to siRNA DDR1 only and siRNA DDR1 + DDR1-GFP. To generate the MDA-MB-231 cell line stably expressing Lifeact-mRuby, cells were transduced at a multiplicity of infection of 10.

Cdc42 activity assay

To detect GTP-active bound Cdc42, MDA-MB-231 transfected with CT or DDR1 #1 siRNA were cultured for 2 h on type I collagen fibrils or overnight on plastic. 50 µg of protein was subjected using the G-LISA Cdc42 Activation Assay Biochem kit (Cytoskeleton, Inc.) according to the manufacturer's instructions.

Gelatin degradation assay

Coverslips were coated with Oregon green gelatin (Invitrogen), fixed with 0.5% glutaraldehyde (Electron Microscopy Sciences), and washed three times with PBS (Invitrogen). Cells were seeded on coated coverslips and incubated overnight before fixation and staining.

Immunofluorescence and imaging

Cells were fixed with 4% paraformaldehyde, pH 7.2, for 10 min, permeabilized with 0.2% Triton X-100 for 10 min, and incubated with various antibodies. Cells were imaged with an SP5 confocal microscope (Leica) using a 63×/NA 1.4 Plan Neofluor objective lens. To prevent contamination between fluorochromes, each channel was imaged sequentially using the multitrack recording module before merging.

Collagen polymerization, linear invadosome quantification, and collagen degradation

Collagen polymerization and linear invadosome quantifications were made as described previously (Juin et al., 2012). In brief, collagen was diluted at 0.5 mg/ml in DPBS 1×, then polymerized for 4 h at 37°C before cell seeding. Cells were seeded for 4 h on collagen before fixation. Confocal images of isolated cells were obtained using an SP5 confocal microscope (Leica) using a 63×/NA 1.4 Plan NeoFluor objective lens. Cell surface area was measured upon phalloidin staining, and Tks5 staining was used as a marker for linear invadosomes. We used a custom macro (macros 1–3, available as supplemental files) with ImageJ software (W. Rasband, National Institutes of Health) that allowed measurement of all required parameters of linear invadosomes: number, size (using the Feret diameter, the longest distance between any two points), and area (A.U.). Collagen degradation using the anti–collagen type I cleavage site antibody (rabbit, Col1 3/4 short C) was done using a custom macro (see supplemental files) with ImageJ.

SHG imaging of collagen fibers and quantification

The SHG imaging system consists of a confocal TCS SP2 scanning head (Leica) mounted on an inverted microscope (DMIRE2; Leica) and equipped with a MAITAI femtosecond laser (Spectra Physics). A 10× dry objective lens (NA 0.4; Leica) was used for applying an 820-nm excitation to the sample. The SHG signal was collected in the forward direction using the condenser (S1, NA = 0.9–1.4; Leica), and the two-photon-excited fluorescence (TPEF) was epi-collected in the backward direction. IRSP 715 band-pass and 410-nm infrared (IR) filters (10-nm full width at half-maximum [FWHM]) were placed before the photomultiplier tube.

All image analysis was performed with the ImageJ software, using a custom macro (see supplemental files). For collagen quantification, SHG images were thresholded and the mean pixel numbers corresponding to collagen were converted to square micrometers, multiplying by a factor of 8.583 and taking into account the point spread function of the objective. For cell counts, the TPEF images were thresholded and watersheded before performing the "Analyze Particles" function.

Invasion assay

The invasion assay was adapted from Lopez et al. (2005). 1 mg/ml type I rat tail collagen (BD) was used. Costar Transwell inserts (8-µm pore; Corning) and gels were allowed to polymerize at 37°C for 1 h. Collagen gel matrices were then hydrated with DMEM (Life Technologies) supplemented with 50% fetal bovine serum (Biomedia) for 4 h. Cells were washed twice in serum-free medium, trypsinized, counted, placed in the upper chamber of the Transwell insert, and allowed to invade for the indicated time points. After invasion, the Transwell inserts were removed from the plate and the quantity of invading cells into the gel matrix was determined by F-actin staining.

Western blotting and immunoprecipitation

Cells were lysed in radio-immunoprecipitation assay buffer (25 mM Tris HCl, pH 7.5, 150 mM NaCl, 1% IGEPAL, 1% sodium deoxycholate, and 0.1% SDS), sonicated, incubated at 95°C for 5 min, and loaded onto a

10% or 12% SDS-PAGE gel. Proteins were blotted onto a nitrocellulose membrane (Sigma-Aldrich), blocked with 5% bovine serum albumin, and probed with primary antibody overnight. Membranes were then washed and incubated with the corresponding secondary antibody, and signals were acquired and quantified with the Odyssey system (LI-COR Biosciences).

Biosensor assay and FRET analysis

Raichu-Cdc42 biosensor was used for FRET imaging to measure Cdc42 activity (Aoki and Matsuda, 2009). MDA-MB-231 cells transfected with the biosensor were plated in µ-Dish 35 mm, high glass bottom plates (Ibidi) coated with type I collagen. 2 h later, living cells were imaged using an inverted microscope (TE Eclipse; Nikon) equipped with a motorized heated and CO_2-regulated incubator. Images were taken using a Nikon 100× Plan-Apochromat VC 1.4 oil objective lens and captured with an EM charge-coupled device (CCD) camera (C9100-13, ImagEM; Hamamatsu Photonics) controlled by the MetaMorph 7.0 software. A ratio image of YPF/CFP was created to represent FRET efficiency, which correlated with the activities of the G proteins. Pseudocolored ratio images were generated from images of CFP and FRET channels, as described previously (Hodgson et al., 2006). For quantification, the frequency of colocalization between active probe and collagen I fibrils was observed and presented as the number of cells presenting active probe on collagen I fibrils per number of cells observed (two independent experiments).

Video microscopy

MDA-MB-231 cells stably expressing Lifeact-mRuby were transfected with pTks5-GFP construction. The next day after transfection, cells were plated on 14-mm glass-bottom dishes, No. 1.5 thickness (MatTek) before being coated with 633 fluorescent collagen type I. Cells were imaged 2 h after seeding, with or without PP2 in DMEM 4.5 g/liter glucose, Hepes, no phenol red, and 10% fetal calf serum at 37°C without CO_2. A picture was taken every 4 min for 1 h with a confocal microscope (SP5; Leica).

Colocalization quantification

For colocalization quantification, we used Co-localization Finder Version 1.2 from C. Laummonerie and J. Mutterer (Institut de Biologie Moleculaire des Plantes, Strasbourg, France) on ImageJ version 1.48. Results were presented as the mean of 10 fields quantified.

Statistical tests

Data were reported as the mean ± SEM of at least three experiments. Statistical significance ($P < 0.05$ or less) was determined using a paired *t* test or analysis of variance (ANOVA) as appropriate and performed with GraphPad Prism software (GraphPad Software).

Online supplemental material

Fig. S1 demonstrates the impact of type I collagen fibrils on cell degradation activity and confirms the DDR1 localization with linear invadosomes. Fig. S2 reveals DDR1 involvement in linear invadosome formation in A549 cells and shows a rescue experiment on cells depleted for DDR1 and infected with DDR1-GFP. Fig. S3 describes the DDR1 role in classical invadosome formation and activity. Figs. S4 and S5 demonstrate that the role of DDR1 in collagen degradation and cell invasion is MMP dependent but Src independent. Table S1 contains the list of siRNAs tested to screen for GEFs involved in linear invadosome formation. Video 1 shows the dynamics of Tks5-GFP and F-actin on MDA-MB-231 cells seeded on labeled type I collagen fibrils. ImageJ macros 1 and 2 were used to determine the number and the size of linear invadosomes per cell and collagen degradation. ImageJ macro3 was used to quantify SHG signal. Online supplemental material is available at http://www.jcb.org/cgi/content/full/jcb.201404079/DC1.

We are grateful to Dr. A. Wiedmann and Dr. C. Perret for the SYF and Huh6 cell lines, respectively. We thank Drs. S. Courtneidge, P. De Camilli, M. Bendeck, R. Wedlich-Soeldner, G. Longmore, and M. Matsuda for constructs. We thank the Bordeaux Imaging Center for help with fluorescence quantification (BIC) and P. Chavrier and A. Blangy for helpful discussions.

A. Juin is supported by a predoctoral fellowship from the Ministère de l'Enseignement Supérieur et de la Recherche. J. Di Martino is supported by a PhD fellowship from Institut National de la Santé et de la Recherche Médicale/Région Aquitaine. L. Paysan is supported by a PhD fellowship from Région Aquitaine. E. Henriet is supported by a PhD from the Ministère de l'Enseignement Supérieur et de la Recherche. This work was supported by grants from ANR-13-JJC-JSV1-0005, l'AFEF (Association Française pour l'Etude du Foie), La Ligue Nationale contre le Cancer, and Association pour la Recherche sur le Cancer. V. Moreau and J. Rosenbaum are supported by funding from Equipe Labellisée Ligue Nationale contre le Cancer 2011 and Grant Institut National du Cancer - Direction Générale de l'Offre de Soins - Institut National de la Santé et de la Recherche Médicale 6046.

The authors declare no competing financial interests.

Submitted: 14 April 2014
Accepted: 21 October 2014

References

Albiges-Rizo, C., O. Destaing, B. Fourcade, E. Planus, and M.R. Block. 2009. Actin machinery and mechanosensitivity in invadopodia, podosomes, and focal adhesions. *J. Cell Sci.* 122:3037–3049. http://dx.doi.org/10.1242/jcs.052704

Angers-Loustau, A., R. Hering, T.E. Werbowetski, D.R. Kaplan, and R.F. Del Maestro. 2004. SRC regulates actin dynamics and invasion of malignant glial cells in three dimensions. *Mol. Cancer Res.* 2:595–605.

Aoki, K., and M. Matsuda. 2009. Visualization of small GTPase activity with fluorescence resonance energy transfer-based biosensors. *Nat. Protoc.* 4:1623–1631. http://dx.doi.org/10.1038/nprot.2009.175

Ayala, I., G. Giacchetti, G. Caldieri, F. Attanasio, S. Mariggiò, S. Tetè, R. Polishchuk, V. Castronovo, and R. Buccione. 2009. Faciogenital dysplasia protein Fgd1 regulates invadopodia biogenesis and extracellular matrix degradation and is up-regulated in prostate and breast cancer. *Cancer Res.* 69:747–752. http://dx.doi.org/10.1158/0008-5472.CAN-08-1980

Azzam, H.S., and E.W. Thompson. 1992. Collagen-induced activation of the M(r) 72,000 type IV collagenase in normal and malignant human fibroblastoid cells. *Cancer Res.* 52:4540–4544.

Barker, K.T., J.E. Martindale, P.J. Mitchell, T. Kamalati, M.J. Page, D.J. Phippard, T.C. Dale, B.A. Gusterson, and M.R. Crompton. 1995. Expression patterns of the novel receptor-like tyrosine kinase, DDR, in human breast tumours. *Oncogene*. 10:569–575.

Beaty, B.T., V.P. Sharma, J.J. Bravo-Cordero, M.A. Simpson, R.J. Eddy, A.J. Koleske, and J. Condeelis. 2013. β1 integrin regulates Arg to promote invadopodial maturation and matrix degradation. *Mol. Biol. Cell*. 24:1661–1675: S1–S11. http://dx.doi.org/10.1091/mbc.E12-12-0908

Carafoli, F., M.C. Mayer, K. Shiraishi, M.A. Pecheva, L.Y. Chan, R. Nan, B. Leitinger, and E. Hohenester. 2012. Structure of the discoidin domain receptor 1 extracellular region bound to an inhibitory Fab fragment reveals features important for signaling. *Structure*. 20:688–697. http://dx.doi.org/10.1016/j.str.2012.02.011

Cestra, G., A. Kwiatkowski, M. Salazar, F. Gertler, and P. De Camilli. 2005. Tuba, a GEF for CDC42, links dynamin to actin regulatory proteins. *Methods Enzymol.* 404:537–545. http://dx.doi.org/10.1016/S0076-6879(05)04047-4

Cook, D.R., K.L. Rossman, and C.J. Der. 2014. Rho guanine nucleotide exchange factors: regulators of Rho GTPase activity in development and disease. *Oncogene*. 33:4021–4035. http://dx.doi.org/10.1038/onc.2013.362

Cox, T.R., D. Bird, A.M. Baker, H.E. Barker, M.W. Ho, G. Lang, and J.T. Erler. 2013. LOX-mediated collagen crosslinking is responsible for fibrosis-enhanced metastasis. *Cancer Res.* 73:1721–1732. http://dx.doi.org/10.1158/0008-5472.CAN-12-2233

Day, E., B. Waters, K. Spiegel, T. Alnadaf, P.W. Manley, E. Buchdunger, C. Walker, and G. Jarai. 2008. Inhibition of collagen-induced discoidin domain receptor 1 and 2 activation by imatinib, nilotinib and dasatinib. *Eur. J. Pharmacol.* 599:44–53. http://dx.doi.org/10.1016/j.ejphar.2008.10.014

Dejmek, J., K. Dib, M. Jönsson, and T. Andersson. 2003. Wnt-5a and G-protein signaling are required for collagen-induced DDR1 receptor activation and normal mammary cell adhesion. *Int. J. Cancer*. 103:344–351. http://dx.doi.org/10.1002/ijc.10752

Dejmek, J., K. Leandersson, J. Manjer, A. Bjartell, S.O. Emdin, W.F. Vogel, G. Landberg, and T. Andersson. 2005. Expression and signaling activity of Wnt-5a/discoidin domain receptor-1 and Syk plays distinct but decisive roles in breast cancer patient survival. *Clin. Cancer Res.* 11:520–528.

Deroanne, C., V. Vouret-Craviari, B. Wang, and J. Pouysségur. 2003. EphrinA1 inactivates integrin-mediated vascular smooth muscle cell spreading via the Rac/PAK pathway. *J. Cell Sci.* 116:1367–1376. http://dx.doi.org/10.1242/jcs.00308

Destaing, O., E. Planus, D. Bouvard, C. Oddou, C. Badowski, V. Bossy, A. Raducanu, B. Fourcade, C. Albiges-Rizo, and M.R. Block. 2010. β1A integrin is a master regulator of invadosome organization and function. *Mol. Biol. Cell*. 21:4108–4119. http://dx.doi.org/10.1091/mbc.E10-07-0580

Destaing, O., M.R. Block, E. Planus, and C. Albiges-Rizo. 2011. Invadosome regulation by adhesion signaling. *Curr. Opin. Cell Biol.* 23:597–606. http://dx.doi.org/10.1016/j.ceb.2011.04.002

Di Martino, J., L. Paysan, C. Gest, V. Lagrée, A. Juin, F. Saltel, and V. Moreau. 2014. Cdc42 and Tks5: A minimal and universal molecular signature

for functional invadosomes. *Cell Adhes. Migr.* 8:280–292. http://dx.doi.org/10.4161/cam.28833

Eckert, M.A., T.M. Lwin, A.T. Chang, J. Kim, E. Danis, L. Ohno-Machado, and J. Yang. 2011. Twist1-induced invadopodia formation promotes tumor metastasis. *Cancer Cell*. 19:372–386. http://dx.doi.org/10.1016/j.ccr.2011.01.036

Ford, C.E., S.K. Lau, C.Q. Zhu, T. Andersson, M.S. Tsao, and W.F. Vogel. 2007. Expression and mutation analysis of the discoidin domain receptors 1 and 2 in non-small cell lung carcinoma. *Br. J. Cancer*. 96:808–814. http://dx.doi.org/10.1038/sj.bjc.6603614

Gailhouste, L., Y. Le Grand, C. Odin, D. Guyader, B. Turlin, F. Ezan, Y. Désille, T. Guilbert, A. Bessard, C. Frémin, et al. 2010. Fibrillar collagen scoring by second harmonic microscopy: a new tool in the assessment of liver fibrosis. *J. Hepatol.* 52:398–406. http://dx.doi.org/10.1016/j.jhep.2009.12.009

Gilkes, D.M., P. Chaturvedi, S. Bajpai, C.C. Wong, H. Wei, S. Pitcairn, M.E. Hubbi, D. Wirtz, and G.L. Semenza. 2013. Collagen prolyl hydroxylases are essential for breast cancer metastasis. *Cancer Res.* 73:3285–3296. http://dx.doi.org/10.1158/0008-5472.CAN-12-3963

Grise, F., S. Sena, A. Bidaud-Meynard, J. Baud, J.B. Hiriart, K. Makki, N. Dugot-Senant, C. Staedel, P. Bioulac-Sage, J. Zucman-Rossi, et al. 2012. Rnd3/RhoE Is down-regulated in hepatocellular carcinoma and controls cellular invasion. *Hepatology*. 55:1766–1775. http://dx.doi.org/10.1002/hep.25568

Hauck, C.R., D.A. Hsia, D. Ilic, and D.D. Schlaepfer. 2002. v-Src SH3-enhanced interaction with focal adhesion kinase at β1 integrin-containing invadopodia promotes cell invasion. *J. Biol. Chem.* 277:12487–12490. http://dx.doi.org/10.1074/jbc.C100760200

Hidalgo-Carcedo, C., S. Hooper, S.I. Chaudhry, P. Williamson, K. Harrington, B. Leitinger, and E. Sahai. 2011. Collective cell migration requires suppression of actomyosin at cell-cell contacts mediated by DDR1 and the cell polarity regulators Par3 and Par6. *Nat. Cell Biol.* 13:49–58. http://dx.doi.org/10.1038/ncb2133

Hodgson, L., P. Nalbant, F. Shen, and K. Hahn. 2006. Imaging and photobleach correction of Mero-CBD, sensor of endogenous Cdc42 activation. *Methods Enzymol*. 406:140–156. http://dx.doi.org/10.1016/S0076-6879(06)06012-5

Hoshino, D., K.M. Branch, and A.M. Weaver. 2013. Signaling inputs to invadopodia and podosomes. *J. Cell Sci.* 126:2979–2989. http://dx.doi.org/10.1242/jcs.079475

Itoh, R.E., K. Kurokawa, Y. Ohba, H. Yoshizaki, N. Mochizuki, and M. Matsuda. 2002. Activation of rac and cdc42 video imaged by fluorescent resonance energy transfer-based single-molecule probes in the membrane of living cells. *Mol. Cell. Biol.* 22:6582–6591. http://dx.doi.org/10.1128/MCB.22.18.6582-6591.2002

Juin, A., C. Billottet, V. Moreau, O. Destaing, C. Albiges-Rizo, J. Rosenbaum, E. Génot, and F. Saltel. 2012. Physiological type I collagen organization induces the formation of a novel class of linear invadosomes. *Mol. Biol. Cell*. 23:297–309. http://dx.doi.org/10.1091/mbc.E11-07-0594

Klinghoffer, R.A., C. Sachsenmaier, J.A. Cooper, and P. Soriano. 1999. Src family kinases are required for integrin but not PDGFR signal transduction. *EMBO J.* 18:2459–2471. http://dx.doi.org/10.1093/emboj/18.9.2459

Konitsiotis, A.D., N. Raynal, D. Bihan, E. Hohenester, R.W. Farndale, and B. Leitinger. 2008. Characterization of high affinity binding motifs for the discoidin domain receptor DDR2 in collagen. *J. Biol. Chem.* 283:6861–6868. http://dx.doi.org/10.1074/jbc.M709290200

Koo, D.H., C. McFadden, Y. Huang, R. Abdulhussein, M. Friese-Hamim, and W.F. Vogel. 2006. Pinpointing phosphotyrosine-dependent interactions downstream of the collagen receptor DDR1. *FEBS Lett.* 580:15–22. http://dx.doi.org/10.1016/j.febslet.2005.11.035

Kovacs, E.M., R.S. Makar, and F.B. Gertler. 2006. Tuba stimulates intracellular N-WASP-dependent actin assembly. *J. Cell Sci.* 119:2715–2726. http://dx.doi.org/10.1242/jcs.03005

Leitinger, B. 2011. Transmembrane collagen receptors. *Annu. Rev. Cell Dev. Biol.* 27:265–290. http://dx.doi.org/10.1146/annurev-cellbio-092910-154013

Leitinger, B. 2014. Discoidin domain receptor functions in physiological and pathological conditions. *Int. Rev. Cell Mol. Biol*. 310:39–87. http://dx.doi.org/10.1016/B978-0-12-800180-6.00002-5

Leong, H.S., A.E. Robertson, K. Stoletov, S.J. Leith, C.A. Chin, A.E. Chien, M.N. Hague, A. Ablack, K. Carmine-Simmen, V.A. McPherson, et al. 2014. Invadopodia are required for cancer cell extravasation and are a therapeutic target for metastasis. *Cell Reports*. 8:1558–1570. http://dx.doi.org/10.1016/j.celrep.2014.07.050

Levental, K.R., H. Yu, L. Kass, J.N. Lakins, M. Egeblad, J.T. Erler, S.F. Fong, K. Csiszar, A. Giaccia, W. Weninger, et al. 2009. Matrix crosslinking forces tumor progression by enhancing integrin signaling. *Cell*. 139:891–906. http://dx.doi.org/10.1016/j.cell.2009.10.027

Linder, S., K. Hüfner, U. Wintergerst, and M. Aepfelbacher. 2000. Microtubule-dependent formation of podosomal adhesion structures in primary human macrophages. *J. Cell Sci.* 113:4165–4176.

Linder, S., C. Wiesner, and M. Himmel. 2011. Degrading devices: invadosomes in proteolytic cell invasion. *Annu. Rev. Cell Dev. Biol.* 27:185–211. http://dx.doi.org/10.1146/annurev-cellbio-092910-154216

Lopez, J.I., T.D. Camenisch, M.V. Stevens, B.J. Sands, J. McDonald, and J.A. Schroeder. 2005. CD44 attenuates metastatic invasion during breast cancer progression. *Cancer Res.* 65:6755–6763. http://dx.doi.org/10.1158/0008-5472.CAN-05-0863

Miao, L., S. Zhu, Y. Wang, Y. Li, J. Ding, J. Dai, H. Cai, D. Zhang, and Y. Song. 2013. Discoidin domain receptor 1 is associated with poor prognosis of non-small cell lung cancer and promotes cell invasion via epithelial-to-mesenchymal transition. *Med. Oncol.* 30:626. http://dx.doi.org/10.1007/s12032-013-0626-4

Monteiro, P., C. Rossé, A. Castro-Castro, M. Irondelle, E. Lagoutte, P. Paul-Gilloteaux, C. Desnos, E. Formstecher, F. Darchen, D. Perrais, et al. 2013. Endosomal WASH and exocyst complexes control exocytosis of MT1-MMP at invadopodia. *J. Cell Biol.* 203:1063–1079. http://dx.doi.org/10.1083/jcb.201306162

Moreau, V., F. Tatin, C. Varon, and E. Génot. 2003. Actin can reorganize into podosomes in aortic endothelial cells, a process controlled by Cdc42 and RhoA. *Mol. Cell. Biol.* 23:6809–6822. http://dx.doi.org/10.1128/MCB.23.19.6809-6822.2003

Murphy, D.A., and S.A. Courtneidge. 2011. The 'ins' and 'outs' of podosomes and invadopodia: characteristics, formation and function. *Nat. Rev. Mol. Cell Biol.* 12:413–426. http://dx.doi.org/10.1038/nrm3141

Rajabian, T., B. Gavicherla, M. Heisig, S. Müller-Altrock, W. Goebel, S.D. Gray-Owen, and K. Ireton. 2009. The bacterial virulence factor InlC perturbs apical cell junctions and promotes cell-to-cell spread of Listeria. *Nat. Cell Biol.* 11:1212–1218. http://dx.doi.org/10.1038/ncb1964

Ramaswamy, S., K.N. Ross, E.S. Lander, and T.R. Golub. 2003. A molecular signature of metastasis in primary solid tumors. *Nat. Genet.* 33:49–54. http://dx.doi.org/10.1038/ng1060

Razidlo, G.L., B. Schroeder, J. Chen, D.D. Billadeau, and M.A. McNiven. 2014. Vav1 as a central regulator of invadopodia assembly. *Curr. Biol.* 24:86–93. http://dx.doi.org/10.1016/j.cub.2013.11.013

Riedl, J., K.C. Flynn, A. Raducanu, F. Gärtner, G. Beck, M. Bösl, F. Bradke, S. Massberg, A. Aszodi, M. Sixt, and R. Wedlich-Söldner. 2010. Lifeact mice for studying F-actin dynamics. *Nat. Methods*. 7:168–169. http://dx.doi.org/10.1038/nmeth0310-168

Ruangpanit, N., D. Chan, K. Holmbeck, H. Birkedal-Hansen, J. Polarek, C. Yang, J.F. Bateman, and E.W. Thompson. 2001. Gelatinase A (MMP-2) activation by skin fibroblasts: dependence on MT1-MMP expression and fibrillar collagen form. *Matrix Biol.* 20:193–203. http://dx.doi.org/10.1016/S0945-053X(01)00135-4

Salazar, M.A., A.V. Kwiatkowski, L. Pellegrini, G. Cestra, M.H. Butler, K.L. Rossman, D.M. Serna, J. Sondek, F.B. Gertler, and P. De Camilli. 2003. Tuba, a novel protein containing bin/amphiphysin/Rvs and Dbl homology domains, links dynamin to regulation of the actin cytoskeleton. *J. Biol. Chem.* 278:49031–49043. http://dx.doi.org/10.1074/jbc.M308104200

Sato, K., S. Hattori, S. Irie, and S. Kawashima. 2003. Spike formation by fibroblasts adhering to fibrillar collagen I gel. *Cell Struct. Funct.* 28:229–241. http://dx.doi.org/10.1247/csf.28.229

Schachtner, H., S.D. Calaminus, A. Sinclair, J. Monypenny, M.P. Blundell, C. Leon, T.L. Holyoake, A.J. Thrasher, A.M. Michie, M. Vukovic, et al. 2013. Megakaryocytes assemble podosomes that degrade matrix and protrude through basement membrane. *Blood*. 121:2542–2552. http://dx.doi.org/10.1182/blood-2012-07-443457

Shintani, Y., Y. Fukumoto, N. Chaika, R. Svoboda, M.J. Wheelock, and K.R. Johnson. 2008. Collagen I-mediated up-regulation of N-cadherin requires cooperative signals from integrins and discoidin domain receptor 1. *J. Cell Biol.* 180:1277–1289. http://dx.doi.org/10.1083/jcb.200708137

Shrivastava, A., C. Radziejewski, E. Campbell, L. Kovac, M. McGlynn, T.E. Ryan, S. Davis, M.P. Goldfarb, D.J. Glass, G. Lemke, and G.D. Yancopoulos. 1997. An orphan receptor tyrosine kinase family whose members serve as nonintegrin collagen receptors. *Mol. Cell*. 1:25–34. http://dx.doi.org/10.1016/S1097-2765(00)80004-0

Takino, T., H. Miyamori, Y. Watanabe, K. Yoshioka, M. Seiki, and H. Sato. 2004. Membrane type 1 matrix metalloproteinase regulates collagen-dependent mitogen-activated protein/extracellular signal-related kinase activation and cell migration. *Cancer Res.* 64:1044–1049. http://dx.doi.org/10.1158/0008-5472.CAN-03-1843

Tarone, G., D. Cirillo, F.G. Giancotti, P.M. Comoglio, and P.C. Marchisio. 1985. Rous sarcoma virus-transformed fibroblasts adhere primarily at discrete protrusions of the ventral membrane called podosomes. *Exp. Cell Res.* 159:141–157. http://dx.doi.org/10.1016/S0014-4827(85)80044-6

Valencia, K., C. Ormazábal, C. Zandueta, D. Luis-Ravelo, I. Antón, M.J. Pajares, J. Agorreta, L.M. Montuenga, S. Martínez-Canarias, B. Leitinger, and F. Lecanda. 2012. Inhibition of collagen receptor discoidin domain receptor-1 (DDR1) reduces cell survival, homing, and colonization in lung cancer bone metastasis. *Clin. Cancer Res.* 18:969–980. http://dx.doi.org/10.1158/1078-0432.CCR-11-1686

Valiathan, R.R., M. Marco, B. Leitinger, C.G. Kleer, and R. Fridman. 2012. Discoidin domain receptor tyrosine kinases: new players in cancer progression. *Cancer Metastasis Rev.* 31:295–321. http://dx.doi.org/10.1007/s10555-012-9346-z

Vogel, W., G.D. Gish, F. Alves, and T. Pawson. 1997. The discoidin domain receptor tyrosine kinases are activated by collagen. *Mol. Cell.* 1:13–23. http://dx.doi.org/10.1016/S1097-2765(00)80003-9

Wolf, K., M. Te Lindert, M. Krause, S. Alexander, J. Te Riet, A.L. Willis, R.M. Hoffman, C.G. Figdor, S.J. Weiss, and P. Friedl. 2013. Physical limits of cell migration: control by ECM space and nuclear deformation and tuning by proteolysis and traction force. *J. Cell Biol.* 201:1069–1084. http://dx.doi.org/10.1083/jcb.201210152

Xu, H., D. Bihan, F. Chang, P.H. Huang, R.W. Farndale, and B. Leitinger. 2012. Discoidin domain receptors promote $\alpha1\beta1$- and $\alpha2\beta1$-integrin mediated cell adhesion to collagen by enhancing integrin activation. *PLoS ONE.* 7:e52209. http://dx.doi.org/10.1371/journal.pone.0052209

Yang, K., J.H. Kim, H.J. Kim, I.S. Park, I.Y. Kim, and B.S. Yang. 2005. Tyrosine 740 phosphorylation of discoidin domain receptor 2 by Src stimulates intramolecular autophosphorylation and Shc signaling complex formation. *J. Biol. Chem.* 280:39058–39066. http://dx.doi.org/10.1074/jbc.M506921200

Yang, S.H., H.A. Baek, H.J. Lee, H.S. Park, K.Y. Jang, M.J. Kang, D.G. Lee, Y.C. Lee, W.S. Moon, and M.J. Chung. 2010. Discoidin domain receptor 1 is associated with poor prognosis of non-small cell lung carcinomas. *Oncol. Rep.* 24:311–319.

Yeh, Y.C., C.Z. Wang, and M.J. Tang. 2009. Discoidin domain receptor 1 activation suppresses $\alpha_2\beta_1$ integrin-dependent cell spreading through inhibition of Cdc42 activity. *J. Cell. Physiol.* 218:146–156. http://dx.doi.org/10.1002/jcp.21578

Zhang, K., C.A. Corsa, S.M. Ponik, J.L. Prior, D. Piwnica-Worms, K.W. Eliceiri, P.J. Keely, and G.D. Longmore. 2013. The collagen receptor discoidin domain receptor 2 stabilizes SNAIL1 to facilitate breast cancer metastasis. *Nat. Cell Biol.* 15:677–687. http://dx.doi.org/10.1038/ncb2743